



PESTIPOND: A descriptive model of pesticide fate in artificial ponds: II. Model application and evaluation

Aya Bahi, Sabine Sauvage, Sylvain Payraudeau, Julien Tournebize

► To cite this version:

Aya Bahi, Sabine Sauvage, Sylvain Payraudeau, Julien Tournebize. PESTIPOND: A descriptive model of pesticide fate in artificial ponds: II. Model application and evaluation. *Ecological Modelling*, 2023, 484, pp.110472. 10.1016/j.ecolmodel.2023.110472 . hal-04191025

HAL Id: hal-04191025

<https://hal.inrae.fr/hal-04191025>

Submitted on 30 Aug 2023

HAL is a multi-disciplinary open access archive for the deposit and dissemination of scientific research documents, whether they are published or not. The documents may come from teaching and research institutions in France or abroad, or from public or private research centers.

L'archive ouverte pluridisciplinaire **HAL**, est destinée au dépôt et à la diffusion de documents scientifiques de niveau recherche, publiés ou non, émanant des établissements d'enseignement et de recherche français ou étrangers, des laboratoires publics ou privés.

PESTIPOND: A descriptive model of pesticide fate in artificial ponds: II. Model application and evaluation

Aya Bahi^{a}, Sabine Sauvage^b, Sylvain Payraudeau^c, Julien Tournebize^{a*}*

^a INRAE, French National Research Institute for Agriculture, Food and the Environment, University of Paris-Saclay, CS 10030, F-92761 Antony, France

^b Laboratory of functional Ecology and Environment, University of Toulouse, CNRS, UPS, Toulouse INP, ENSAT campus, F-31326 Toulouse, France

^c ITES, Institut Terre et Environnement de Strasbourg (ITES), University of Strasbourg /ENGEEES, CNRS UMR 7063, F-67084 Strasbourg, France

* Corresponding authors.

E-mail addresses aya.bahi@inrae.fr; julien.tournebize@inrae.fr

Abstract

Some artificial ponds (APs) are designed to collect part of the agricultural water fluxes and dissipate their pesticide contamination through a synergy of physicochemical processes. APs act as buffer zones and mitigate pesticide transfer of farm plots to natural water resources. As part of a two-paper series, this paper addresses the application and validation of the PESTIPOND model. PESTIPOND is a process-based model developed to predict pesticides' behavior and distribution in APs located in drained agricultural catchments. The development and sensitivity analysis of the model are described in Paper I (Bahi et al., 2023a). PESTIPOND was applied on the Rampillon AP to characterize the fate of seven different pesticides and five monitoring periods while considering the key transfer and transformation processes. The model was assessed through various methods against the observed data in simulating pesticide dynamics. The statistical and graphical evaluation of PESTIPOND reflected a good performance except for boscalid. The sensitivity analysis and application of the model evidenced that adsorption-desorption and biotransformation in the pond water are major processes behind pesticide dissipation. Hydrophobic and lowly mobile pesticides are more likely to be bio-transformed at the water-sediment interface. This work highlights the link between the hydraulic residential time (HRT), temperature, and APs' efficiency in minimizing pesticide transfer into the environment. The model predicted that the actual efficiency of the AP covering 0.15% of the drained catchment would double if the pond's surface area covered at least 1% of the catchment. Moreover, the model's predictions evidenced that a temperature rise of 10°C will increase the dissipation of pesticides by only 8%. PESTIPOND provides key elements that are useful to design and manage ponds with optimal efficiency. Hence, these APs can be complementary solutions to pesticide use regulation to reduce the transfer of agricultural contamination into freshwater resources.

Keywords:

Pesticide; artificial pond; model; mass budget; dissipation; calibration

1 Introduction

Due to the broad-spectrum toxicity of pesticides, they are a non-point source of pollution for the ecosystem since they are transferred from agricultural plots to natural water resources through surface runoff and subsurface drainage. Pesticides are particularly pernicious for the ecosystem compared to other chemicals because they are specially manufactured to eliminate pests (Ippolito et al., 2015). As such, pesticides are a major risk for terrestrial and aquatic biodiversity (Messelink et al., 2021; Mineau and Whiteside, 2013) and the ecosystem's functioning (Brühl and Zaller, 2021). There is now compelling evidence that certain pesticides exhibit a serious hazard to humans and other life forms, as well as undesired side effects on the environment (Briggs, 2018; Edwards, 2013; Nagy et al., 2020).

Hence, the need to reduce pesticide inputs into water resources, as they are substantial drinking water supplies and aquatic habitats (Leenhardt et al., 2022). Pesticides have been detected in groundwater (Baran et al., 2008; Hunter, 2012), rivers (Montiel-León et al., 2019; Xu et al., 2020), and lakes (Bhardwaj et al., 2019; Kandie et al., 2020), as well as smaller wetlands (Lorenz et al., 2017; Ulrich et al., 2018), making pesticides a major cause for water quality impairment. As complements to pesticide use regulation and management practices, material solutions can be implemented to safeguard the quality of water resources and mitigate pesticide input into water bodies, such as edge-of-field and riparian buffer strips, vegetated ditches, wetlands, and artificial ponds (Vymazal and Brezinova, 2015).

This study focuses on constructed wetlands, especially edge-of-field artificial ponds (APs) since they have the advantages of needing minimal operations and providing wildlife habitat (Sudarsan and Nithiyantham, 2021). APs are also known for their cost-effectiveness and low energy consumption compared to other surface water treatment methods (e.g., coagulation, membrane filtration, ion exchange, photocatalytic degradation, and adsorption on black carbon and activated carbon) (Aungpradit et al., 2007; Fitch, 2014; Kearns et al., 2014; Trepel, 2010). In practice, edge-of-field APs can act as buffer zones since they are constructed downstream agricultural plots and upstream natural water resources. APs can intercept a part of agricultural water, and after important flow events, the water leaving APs can be less pesticide-loaded, and contamination transfer into the environment can be dissipated. Over the past years and in light of the worsening water shortage, the evaluation of APs environmental role has gained significant attention. The efficiency of APs in reducing pesticide transfer into the environment was widely reiterated in literature (Li et al., 2014; Tournebize et al., 2017; Vymazal and Brezinova, 2015; Zhang et al., 2014). APs provide an area for a series of physicochemical processes to dissipate pesticide water contamination.

Modeling is a practical tool to assess the performance of APs and explore the physicochemical processes behind pesticide dissipation in APs. Modeling can be used to improve the efficiency of APs to safeguard water quality. Models of varying levels of complexity have been developed and applied to field data to gain insight into the performance of APs. However, many of these models were dedicated to simulating nutrient behavior (Kalin et al., 2013; Son et al., 2010; Sonavane and Munavalli, 2009), and fewer models were assigned to pesticides. Among pesticide fate models are the risk assessment models such as PRZM (Carsel, 1998) and MACRO (Larsbo and Jarvis, 2003; Larsbo et al., 2005), which simulate pesticide fate in the root zone and macro-porous field soils, respectively, and TOXSWA (Adriaanse, 1996) from the FOCUS group (Tooby, 1999), to model pesticide fate in ditches. These models provide

knowledge about pesticide behavior upstream APs. Nevertheless, little consideration has been devoted to studying pesticides at the pond scale. Existing models such as AGRO-2014 and TOXSWA are computationally costly because they require a significant number of inputs and parameters and depend on other models' outputs (i.e., PRZM). In addition, AGRO-2014 only accounts for hydrophobic pesticides. The lake-pond module of the Soil and Water Assessment Tool (SWAT) can also simulate the fate of pesticides in APs. However, SWAT does not integrate the effect of temperature and desorption and does not consider the kinetic effect of adsorption-desorption, given that these factors are widely reported as key drivers of pesticides fate (Burrows et al., 2002; Cryder et al., 2021; Kadlec and Wallace, 2008; Kaur and Kaur, 2018; Papaevangelou et al., 2017; Vymazal and Brezinova, 2015).

On this basis, a descriptive model of pesticide fate in APs "*PESTIPOND*" was developed. *PESTIPOND* is built upon simple mathematical formulation with a limited number of inputs and parameters. Contrarily to black-box models considering a single decay rate of pesticides, *PESTIPOND* is a process-based model integrating the key processes behind pesticide fate in APs. *PESTIPOND* simulates the fate of different pesticides (hydrophobic and hydrophilic) intercepted through agricultural water and distributed in the surface water and sediment compartments of the AP. The key processes considered by the model are adsorption-desorption, biotransformation in water and sediments, photolysis, hydrolysis, and volatilization. *PESTIPOND* is designed to be implemented in a landscape model in fine (e.g., SWAT model) to predict the transfer of pesticides at the watershed scale.

The model program was coded using the R language. The input data consists of 10 parameters and 6 forcing variables listed in Table A.1. The model was previously tested on a test-case scenario and successfully simulated the mass in water and sediments of dissolved pesticides contained in agricultural drainage water, using arbitrary parameter values and observed data. The development, testing, and sensitivity analysis (SA) of *PESTIPOND* can be found in (Bahi et al., 2023, submitted). A module of *PESTIPOND* is dedicated to the reactive transport of adsorbed pesticides, but due to a lack of observed data, it still needs to be completely validated.

The main hypotheses of the model are summarized hereafter:

- (1) Concentrations of pesticides are spatially uniform in water and sediments because the AP compartments are considered completely mixed reactors. Hence, once pesticides enter a specific compartment, they are instantly mixed with the entire content and distributed uniformly. In practice, after several hours, the pond water becomes perfectly mixed (Alvord and Kadlec, 1996; Pugliese et al., 2020). Besides, the pond heterogeneities responsible for the non-uniformity of concentrations are usually considered in hydraulics-based models (Henine et al., 2022) rather than chemical-based models, e.g., for pesticides (Bahi et al., submitted, (Watanabe and Takagi, 2000b) and nitrates (Hantush et al., 2013; Krone-Davis et al., 2013).
- (2) Vegetation is not considered by the *PESTIPOND* model. Prior investigations have evidenced that the fraction of pesticides collated in plants were often insignificant in APs (< 10%) (Butkovskiy et al., 2021; Pérez et al., 2022; Singh et al., 2021; Wang and Kelly, 2017). Not considering the vegetation implies neglecting its effect on the hydraulic flow (brakes, dead zones). Nonetheless, this choice of hypothesis was motivated by the environmental focus of the model rather than the hydraulic one, hence also the hypothesis (1).

- (3) No advection or diffusion processes are considered by the model for the following reasons; (a) APs are often constructed on a compacted substrate where the infiltration (leaching) is not significant, and the water velocity at the water-sediment interface is too low resulting in a weak hydraulic gradient that limits advection in the sediment layer and the water-sediment interface. In addition, the water velocity in the water column of the evaluated APs is too low to induce advection of pesticides. (b) Several studies showed that the molecular diffusion of diverse pesticides is too low in the water ($\sim 10^{-9} \text{ m}^2 \cdot \text{s}^{-1}$ at 25°C) (Chevallard et al., 2014; Fernández-Pascual et al., 2020; Sarraute et al., 2019).
- (4) PESTIPOND simulates the fate of pesticides in the first cm of sediments designated as the active sediment layer governing pesticide transformation and transport under flooded conditions. Previous in-situ measurements proffered that pesticide residues are not significant beyond 1cm of depth (Inao and Kitamura, 1999; Mahugija et al., 2018; Nyantakyi et al., 2022; Takagi et al., 2012). The pore water of the active sediment layer is included in the water column compartment.
- (5) Transformation and volatilization processes are corrected according to the temperature change during the simulation period.
- (6) Since the fate of metabolites is still poorly documented, PESTIPOND does not consider transformation products.

The present paper addresses the application and validation of the PESTIPOND model regarding the prediction of pesticide fate in APs. The model application and validation were performed based on inputs from monitoring data in the Rampillon AP and parameter values calibrated or extracted from literature. The model was validated upon 19 scenarios, where each scenario corresponds to a specific pesticide and its corresponding monitoring period (Table A.8).

2 Materials and methods

2.1 Study site

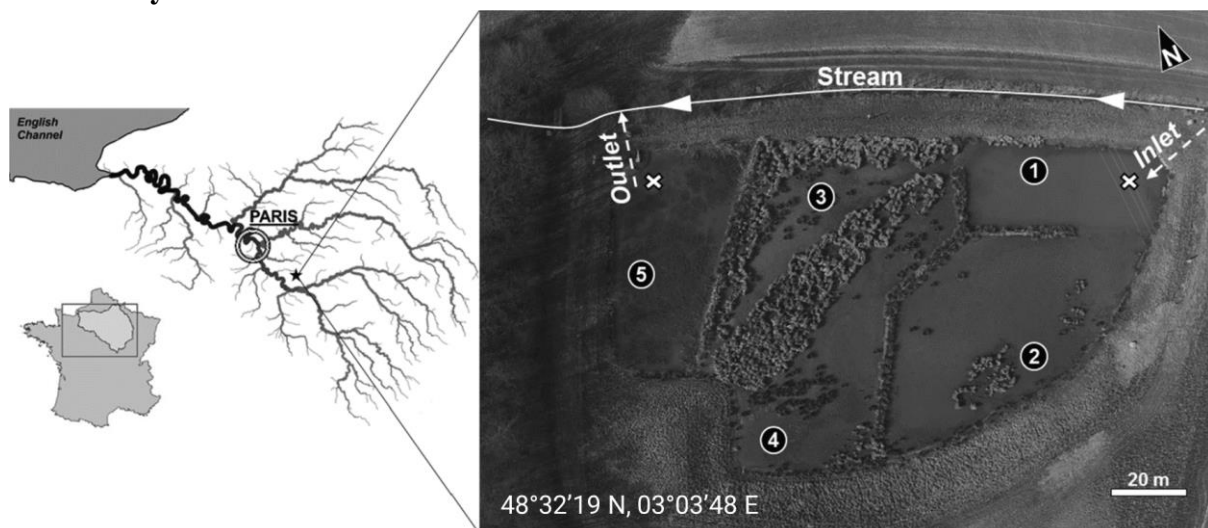


Figure 1: Map visualizing the localization of the AP of Rampillon (Seine-et-Marne, France) within the Seine River basin. Circled numbers indicate the different cells separated by bunds and considered for the spatial sampling (Lebrun et al., 2019). The white arrows refer to the ditch from where the AP intercepts agricultural water.

The experimental set-up is at the Rampillon AP (5270 m^2), located in a 355-ha watershed upstream of the *Ancoeur* agricultural catchment (132.2 km^2), 70 km southeast of Paris, France

(03°03' 37.300E, 48°32'16.700 N) (Fig.1). The AP occupies a 0.15% area of the alimentation watershed and is situated on the Brie plateau subjected to intensive agriculture. The Rampillon AP was implemented in 2010 to address local environmental and health issues (Lebrun et al., 2019; Tournebize et al., 2017; Tournebize et al., 2012). It was designed to collect runoff and drainage water sourcing from agricultural plots before being fed into the Champigny water table, which constitutes a major drinking water resource. Almost 60% of the Champigny water originates from direct infiltration of agricultural runoff through sinkholes (Fig.A.1). The Champigny water table provides drinking water for almost 1.5 million citizens, hence the priority to safeguard its quality by reducing pesticide transfer.

A typical waterlogging French soil characterizes the *Ancoeur* catchment. Therefore, more than 80% of the catchment and the whole Rampillon area have been subsurface drained since 1980 to prevent frequent winter soil saturation (Tournebize et al., 2012). The drains are perforated pipes buried to a depth of 90 m and spaced 10 m apart. The 355-ha watershed receives an annual mean rainfall of 689mm, and the annual mean drained flow is 228 mm. Farmers mainly grow winter wheat, sugar beet, corn, beans, and rape. The Rampillon AP comprises sub-basins separated by bunds to enhance pesticide dissipation and accumulation by increasing the water residence time (HRT) (Tournebize et al., 2012). The first sedimentation basin is 100 cm deep and 300 m³ (Fig.1; i.e., cell 1). The 4000-m² intermediate zone is a shallow sub-basin of a maximum of 50cm deep, including cells 2, 3, and 4 (i.e., 1680, 1450, and 870m², respectively). About 20, 60, and 50% of the inlet and outlet of cells 2, 3, and 4, respectively, were covered by vegetation in 2015: reed (*Phragmites australis*), bulrush (*Juncus* spp.), and sedge (*Carex* spp.). A final 1000-m³ basin, 80 cm deep (i.e., cell 5), was implemented before the outlet. The total volume of the Rampillon pond is 2500 m³. Sediments of the AP are composed of coarse silt for 32.8%, clay for 27.8%, fine sand for 7.7% (3.5%), coarse sand for 2.7% (2%) through a transect from inlet and outlet, and 2-2.8% for organic matter. The loamy texture of sediment is similar to the surrounding soil texture. In 10 years, 10 cm of sediments accumulated in the Rampillon AP. On average, the AP intercepts 40% of the collected drainage water with 30 000 m³ transited per year.

2.2 Monitoring data

The Rampillon AP was initially implemented to buffer nitrate, metals, and pesticides originating from intercepted agricultural water. Therefore, since 2012, the Rampillon AP is instrumented to continuously monitor nutrient and pesticide fluxes and major water physicochemical parameters (i.e., flowrate, temperature, and dominant ions) at the inlet and outlet of the site (Fig.1). The typical monitoring stations comprise a flowmeter based at the water level, a Doppler (Sigma 950, Hach), a multi-parameter spectrophotometer (Spectrolyser UV-vis, S::can) for hourly measurements of turbidity and nitrates, and an automatic sampler managed for bi-monthly flow-weight sampling strategies. IRIS (IRIS Instruments, Orleans, France) also measured water temperature and water level using a pressure transducer model Madofil close to the outlet. Rainfall data were obtained through a local pluviometer installed at the study site. The daily potential evapotranspiration (PET) data are available in the MétéoFrance SAFRAN database (Vidal et al., 2010). PET data values are calculated following the Penman-Monteith formula. The hydrology of the 355-ha watershed is summarized in Fig.A.2. It was chosen to validate the model upon the following five periods: 2014-2015, 2016-2017, 2017-2018, 2018-2019, and 2019-2020 excluding monitoring periods with artifacts and pesticide re-mobilization that is detailed afterward. The selection of the pesticide molecules for

204 the model validation is motivated by the diversity of their chemical properties and their
205 significant detection rate. The monitoring data of the 5270 m² AP during the selected periods
206 are summarized in Table A.8.

207

2.3 Input data

Since 2011, outlet and inlet pesticide concentrations have been monitored in the Rampillon AP. The AP efficiency to mitigate pesticides is calculated from the mass fluxes using Eq.1. Note that the mass flux corresponds to the total mass of pesticide detected in the water with no distinction between the dissolved and particulate fraction.

(1)

$$efficiency (\%) = \left(1 - \frac{outlet\ mass\ flux}{inlet\ mass\ flux}\right) * 100$$

Where the outlet and inlet mass fluxes (μg) are deduced from the concentrations ($\mu\text{g.L}^{-1}$).

Since the rate of pesticide mitigation varies with the type of pesticide, it is suitable to represent the AP performance by a mean efficiency. Fig.A.3 depicts the total efficiency of the Rampillon AP in dissipating each of the seven evaluated in this work. The main physicochemical properties of the evaluated pesticides are listed in Table 1.

The monitoring data showed that, on average, the Rampillon AP dissipates 23% of the total intercepted flux of selected pesticides. The highest dissipation rate (48%) goes to boscalid during 2016-2017, followed by quinmerac (34%) and mesotrione (36%) during 2018-2019. Mesotrione was dissipated by 33% equally during its two years of monitoring, i.e., 2017-2018 and 2018-2019. The mitigation of s-metolachlor varied sharply throughout the years, with a dissipation rate going from 30% during 2016-2017 to 5% during 2014-2015 and 2019-2020. A similar variation was noticed for quinmerac that was dissipated up to 36% during 2018-2019, while its inlet mass was barely reduced during 2014-2015.

Compared to other periods, a significant efficiency was observed during 2016-2017 for bentazon, boscalid, and s-metolachlor. The higher dissipation could result from the high HRT (14 days), and temperature noticed back then (11°C). Similarly, mesotrione and quinmerac were significantly dissipated during 2018-2019, which had an average HRT of 9 days. In fact, a longer HRT provides time for accumulation and transformation processes behind pesticide dissipation, and a higher temperature stimulates the microbial activity behind pesticide biotransformation and is associated with significant solar radiation responsible for photodegradation. This observation ties in with other studies demonstrating that temperature and HRT are major drivers of pesticide behavior in AP (Bahi et al., 2023b; Imfeld et al., 2021; Materu et al., 2021; Pavlidis et al., 2022; Vallée, 2015). Interestingly, mesotrione had a mean dissipation of 50% during a lower mean temperature (9°C) and HRT (7 days). It could be explained by the high biodegradability of the molecule evidenced by short half-lives in both sediment and water, 5.3 and 5.2, respectively (Lewis et al., 2016). These observations underline the potential relationship between pesticide properties, hydro-climatic conditions, and APs performance. Therefore, this relationship will be evaluated using the PESTIPOND model (section 4).

Table 1: The physicochemical properties and the application season of the 7 studied pesticides. K_{oc} (mg.L^{-1}) is the organic carbon-water partition coefficient, representing the mobility of the molecule. $\log K_{ow}$ (-) is the octanol-water partition coefficient, representing the hydrophobicity of the molecule. S (mg.L^{-1}) is the water solubility of the molecule, and LOD ($\mu\text{g.L}^{-1}$) is the detection limit of the molecule in water. The properties values were extracted from literature (Barchanska et al., 2012; Catalá-Icardo et al., 2015; Epa, 2001; Lewis et al., 2016; PubChem, 2021) and the application season was deduced from a follow-up of cultural practices in Rampillon.

Pesticides	K_{oc}	$\log K_{ow}$	S	LOD ($\mu\text{g.L}^{-1}$)
Bentazon	55	2.34	7112	0.005
Boscalid	772	2.96	4.6	0.016
Chlorotoluron	400	2.41	76	0.03
Diiflufenican	550	4.2	0.05	0.07
Mesotrione	122	0.11	1500	0.04-0.61
S-Metolachlor	120	2.9	480	0.02
Quinmerac	86	2.7	107000	0.0006

In terms of the detection frequency of each pesticide, bentazon was the most frequently detected pesticide, which may be due to its wide range of application periods, i.e., March, April, May, and June. Similarly, diiflufenican was highly detected in the Rampillon AP because it was applied during three seasons, i.e., autumn (October and November), winter (January and February), and spring (March). A similar explanation can be accorded to quinmerac applied during autumn (September and October), spring (March, April, and May), and summer (June). On the other hand, Boscalid was only detected during 2014-2015 and 2016-2017. In fact, boscalid was always applied in April and once in May; therefore, if the application did not co-occur with an important spring rainfall event, the pesticide in question would be unlikely to be detected in drainage water. Moreover, due to its K_{oc} (772 L.kg^{-1}) boscalid has a higher affinity to sediments, reducing its availability in the water reaching the pond. Likewise, mesotrione although being applied more frequently, it was only detected twice (2017-2018, 2018-2019). Mesotrione was applied during spring and summer (March, April, and June), with a low incidence of flooding events explaining the molecule's infrequent detection.

The AP efficiencies were calculated based solely on the pond inlet and outlet amount of pesticides. It is; therefore, unknown which processes are driving the dissipation of pesticides. Therefore, the purpose of the PESTIPOND model is to simulate the behavior of pesticides and quantify the contribution of each process to the pesticide fate in APs. Hereafter are detailed the model inputs, i.e., forcing variables and parameters.

2.3.1 Forcing variables

The list of the forcing functions required by the model is provided in Table A.1. It is important to recall that inlet and outlet concentrations are observed bi-monthly at the study site. The concentrations collected each fortnight are the average intercepted concentrations during the past two weeks. Therefore, to have a close insight into pesticide behavior and the model simulations, the bi-monthly observed concentrations were transformed to daily concentrations using a water flow rate weighted interpolation. The transformation method is detailed in (Bahi et al., 2023a). The daily inflow and outflow rates (Q_{in} , Q_{out}) were calculated from the hourly water flow rates measured on-site. The water flow rates are used to compute the inlet and outlet daily mass fluxes from the corresponding concentrations.

M_{in} ($\mu\text{g.d}^{-1}$) and M_{out} ($\mu\text{g.d}^{-1}$) are the daily mass fluxes of the pesticide at the AP's inlet and outlet. C_{in} ($\mu\text{g.L}^{-1}$) and C_{out} ($\mu\text{g.L}^{-1}$) are the daily concentrations at the inlet and outlet of the AP,

respectively. The water volume V_w was computed by the hydrological model detailed in (Bahi et al., 2023a). The hydrological model of PESTIPOND requires daily local rainfall and evaporation data, which were provided by SAFRAN (Vidal et al., 2010), along with the daily temperature T ($^{\circ}\text{C}$), which corresponds to a measurement station nearby the Rampillon AP. The water depth h_w (m) was deduced by Eq.2.

(2)

$$h_w(t) = \frac{V_w(t)}{A}$$

V_w (m^3) is the water volume in the AP, and A (m^2) is the measured surface area of the AP.

2.3.2 Parameters

For the model validation, parameters were either extracted from the pesticide properties database (PPDB) (Lewis et al., 2016) or calibrated, and the AP properties were measured on-site (i.e., (Surface $A=5270 \text{ m}^2$ and the bulk density $\rho_b=0.9 \text{ g.cm}^{-3}$). The temperature correction coefficient θ (see equation in (Bahi et al., 2023a)) is extracted from the literature (Sharifi et al., 2013). The list of the model input parameters is available in Table A.1.

The parameters related to the processes were extracted from the PPDB and calibrated if not available or if calibration would ameliorate the model performance. The calibration was performed manually and numerically using the hydroGOF R-package (Zambrano-Bigiarini, 2020). The R-calibration function seeks the set of parameters leading to the best possible performance of the model according to an evaluation criterion (e.g., NSE and KGE (Eq.3 and Eq.4)).

The model parameters are classified in terms of processes: adsorption-desorption (k_{ads} (d^{-1}) and k_{des} (d^{-1}) for sediment layer) and transformation processes ($DT_{50,w}$, $DT_{50,s}$ and $DT_{50,p}$. A pesticide half-life (DT_{50}) is the time required for the dissipation of 50% of the substance concerned (Gregoire et al., 2009) in water ($DT_{50,w}$), sediments ($DT_{50,s}$), and due to photolysis ($DT_{50,p}$).

The sensitivity analysis results (Bahi et al., 2023, submitted) evidenced that the PESTIPOND model is insensitive to volatilization and hydrolysis independently of the pesticide molecular properties. Therefore, based on literature values (Jacobs and Adriaanse, 2012; Rose et al., 2006), volatilization and hydrolysis rate coefficients were given a fixed value for the rest of the study ($k_v=k_h=10^{-6} \text{ d}^{-1}$), leaving only 5 parameter values to determine ($DT_{50,w}$, $DT_{50,s}$, $DT_{50,p}$, k_{ads} , and k_{des}). The parameter values used to assess the PESTIPOND model are to be found in the result section (section 3).

2.4 Model validation strategy

The validation of the PESTIPOND model is based on the assessment of the simulations of pesticide fluxes against the available observations using the 20 study cases (Table A.8). Other pesticide fate models (Kalin et al., 2013; Watanabe and Takagi, 2000a) were validated using a single pesticide molecule or a single period to evaluate the model performance. Alternatively, PESTIPOND was validated upon field monitoring data of 7 pesticides with contrasting molecular properties (i.e., solubility, hydrophilicity, and mobility) (Table 1) during the 5

evaluated periods. The split-simple test (SST¹) (Klemeš, 1986) is a common evaluation method for this type of model. However, the SST requires sizeable observation data. Even though the monitoring database of the Rampillon AP is consistent (2011-2022), it includes periods of no application nor flooding events responsible for pesticide transfer, which restrains the database size for SST use.

The validation strategy of the PESTIPOND comprises two steps (i) and (ii):

- (i) Based on the observations of pesticide concentrations, the model parameters are optimized for each period (i.e., annual parameters) to assess their stability and consistency. The variability of parameters between periods indicates the degree of the model's robustness.
- (ii) In order to survey the parameters' variability and assess the model robustness, the performance of PESTIPOND is evaluated using a single set of parameters (inter-annual) for all periods (i.e., the mean value of the annual parameters).

Note that for (i) and (ii), the model performance is assessed using both the transformed observations (daily observations) and the non-transformed observations (bi-monthly observations). When the model is validated for the bi-monthly observations, a bi-monthly flow-weighted concentration is calculated from the daily simulation results to match the observations' time scale.

To quantitatively assess model performance, the well-known Nash Sutcliffe efficiency (NSE) objective criterion (Nash and Sutcliffe, 1970) (Eq.3) was adopted. An additional metric was used to assist the NSE criterion, i.e., Kling–Gupta efficiency (KGE) criteria (Gupta et al., 2009) (Eq.4). The two criteria are known for properly evaluating nutrients and chemical fate models (Moriasi et al., 2015). The NSE and KGE values range from $-\infty$ to 1 and require data on both simulated and observed pesticide fluxes. NSE and KGE values close to 1 imply that the model simulations fit the observations owing to good model performance.

The renowned *t*-test (the Student's statistical test) was used to evaluate the similarity between observed and simulated pesticide concentrations (Stokes et al., 2014). Then, a regression analysis was conducted to assess the correlation between the observed and simulated pesticide concentrations (Montgomery et al., 2021). The *t*-test is a hypothesis-based test to compare the means of two groups (e.g., observations and simulations). The test statistics are quantified by the *t*-value (Eq.5) and *p*-value. A low *t*-value indicates a slight difference between the means of both observations and simulations. A *p*-value higher than the significance level ($\alpha=0.05$) means the null hypothesis cannot be rejected (Mishra et al., 2019). The test's null hypothesis is that there is no significant difference between the two groups (Pieri et al., 2007; Serrano, 2012; Wright et al., 2017). To further assess the relationship between observations and simulations, a regression analysis was conducted and quantified by the R^2 (Eq. 6), where *R* is the Bravais-Pearson correlation coefficient (Pearson, 1895; Waldmann, 2019). The higher the R^2 , the more pronounced the correlation between the observed and simulated pesticide concentration. This correlation is statistically significant when the *p*-value of the Pearson test is lower than 0.05. The normalized root means square error (NRMSE) (Eq.7) was also computed to describe the

¹ The split sample test consists in splitting the observation data into two periods. The parameters are calibrated over the first period. Next, the model performance is evaluated by running the calibrated set of parameters obtained over the second period.

discrepancy between the observations and simulations. Since molecules have different concentration ranges, it is statistically more appropriate to compare the NRMSE than the regular RMSE ($\mu\text{g.L}^{-1}$). Therefore, NRMSE was calculated by normalizing the RMSE according to the difference between the maximum and minimum concentrations for each pesticide (Kenney and Keeping, 1962; Sinsomboonthong, 2022). The statistical tests were performed using the “stats” R-package (Lüdtke et al., 2021).

(3)

$$NSE = 1 - \frac{\sum_{t=1}^T (X_t - X_t^*)^2}{\sum_{t=1}^T (X_t^* - \bar{X}_t^*)^2}$$

(4)

$$KGE = 1 - \sqrt{\left(\frac{\text{cov}(X_t^*, X_t)}{\sigma(X_t^*)^2 \sigma(X_t)^2} - 1\right)^2 + \left(\frac{\bar{X}_t}{\bar{X}_t^*} - 1\right)^2 + \left(\frac{\sigma(X_t)}{\sigma(X_t^*)} - 1\right)^2}$$

(5)

$$t = \frac{\bar{X}_t - \bar{X}_t^*}{\sqrt{\frac{\sigma(X_t)}{n} + \frac{\sigma(X_t^*)}{n}}}$$

(6)

$$R^2 = 1 - \frac{\sum (X_t - X_t^*)^2}{\sum (X_t - \bar{X}_t)^2}$$

(7)

$$RMSE = \sqrt{\frac{1}{T} \sum_{t=1}^T (X_t - X_t^*)^2}$$

$$NRMSE = \frac{RMSE}{\max(X_t) - \min(X_t)}$$

Where, X_t^* and X_t correspond to the observations and the simulations at the time step t , respectively. \bar{X}_t^* and \bar{X}_t are the mean values of the observed and simulated pesticide fluxes, respectively, throughout the whole period of interest T . $\text{cov}(X_t^*, X_t)$ refers to the covariance between X_t^* and X_t while σ indicates the standard deviation. n is the size of the observation/simulation sample.

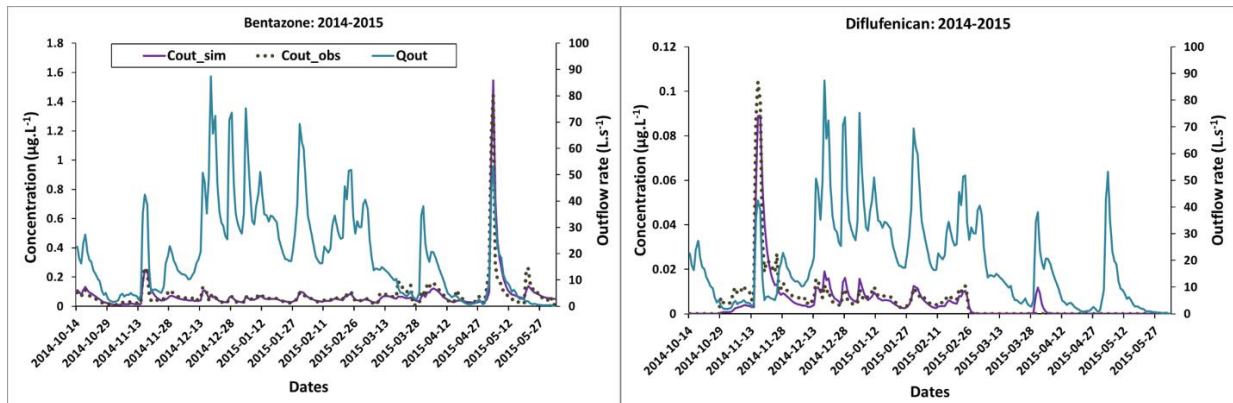
388 3 Results

389 3.1 Model assessment based on the annual calibration

390 An annual calibration of the model parameters according to pesticide fluxes is performed over
391 the selected periods. The obtained parameter values are set out in Tables A.2 & A.3.

392 A graphical and numerical comparison between simulations and observations of pesticide
393 fluxes at the AP outlet were carried out. First, the model performance was assessed according
394 to the daily observations, i.e., the transformed observations from the bi-monthly mean values
395 to daily values (Fig.2). Then according to the bi-monthly observations, i.e., non-transformed
396 observations, while using an annual calibration (Fig.A.5).

397 For brevity and representability, we only exhibit the results of two pesticides during 2014-2015,
398 i.e., the hydrophobic and slightly mobile diflufenican ($K_{oc} \text{ (L.kg}^{-1}) = 550$, $\log K_{ow} = 4.2$) and
399 the hydrophilic and highly mobile bentazon ($K_{oc} \text{ (L.kg}^{-1}) = 55$, $\log K_{ow} = 2.34$) (Lewis et al.,
400 2016) (Fig.2).



401
402 **Figure 2** Graphical comparison of the daily simulations (purple line) and transformed observations (dark points)
403 of the bentazon and diflufenican concentrations in the outlet and the observed outflow rate (blue line).

404 From the graphical (Fig.2) and numerical outcomes (Table 3), it can be noted that the annual
405 calibration results in proper model performance. The KGE and NSE values are >0.5 , and the
406 RMSE does not exceed 0.07. Considering how wide the goodness-of-fit-range of variations are
407 (NSE $(-\infty, 1]$ and KGE $(-\infty, 1]$), the model performance can be considered as “good” due to the
408 annual calibration (Lee et al., 2021; Moriasi et al., 2007; Moriasi et al., 2015).

409
410 The simulations of the daily concentrations and masses of bentazon and diflufenican align with
411 the observations. The outlet concentrations increase after the pesticide application, i.e., during
412 spring for bentazon and autumn for diflufenican (Fig.2). The model simulates the higher
413 exportation of bentazon (40g) in the water compared to diflufenican (3.5g) during 2014-2015.
414 During the same year, quinmerac was also exported significantly, with a total mass of 43g,
415 while the exportation of the other pesticides (i.e., boscalid, chlorotoluron, and s-metolachlor)
416 did not exceed 10g (Fig.A.4).

417
418 However, the model underestimated almost equally the overall exportation of s-metolachlor
419 and quinmerac with a discrepancy of 3g, which covers 5% and 22% of the total intercepted
420 mass, respectively, during 2014-2015. For the rest of the periods and pesticides, the model

managed to reproduce the observed mass exportation. Fig.A.4 displays that the model simulated the lower AP efficiency in dissipating the mass of mesotrione, s-metolachlor, and quinmerac during 2017-2018. During the same year, PESTIPOND also simulates the highest exportation for s-metolachlor (300g). Globally, the simulation results reflect a lower performance at higher concentrations following pesticide applications compared to lower concentrations (Fig.2).

The results underline that the simulations with the annually calibrated set of parameters also fit the non-transformed observations (bi-monthly) of pesticide concentrations (Fig.A.5). The simulated concentration of s-metolachlor was underestimated compared to the observations of two samplings (22/05/2017 and 19/05/2020). Similar underestimation was noted for s-metolachlor mass exportation in Fig.A.4, which is also translated by its lower KGE (0.53) compared to other pesticides (Table 3). Conversely, the model overestimated the concentration of boscalid during 2014-2015 and 2016-2017. This overestimation also concerned the exported boscalid mass during 22/02/2017-20/03/2017 and 22/02/2017 (Fig.A.4). Accordingly, boscalid had the lowest KGE (0.44) (Table 3).

On average, an annual parameter calibration induces a discrepancy between simulated and observed fluxes of 0.03g, all periods and pesticides included. Overall, the graphical comparison evidences the ability of the model to predict the dynamics of the outlet concentrations (Fig.2), and to simulate the concentrations observed in the field (Fig.A.5). The KGE and NSE criteria reflect a good performance of the PESTIPOND model according to the annual calibration, except for boscalid (Table 3).

3.2 Model assessment based on the inter-annual calibration

The adsorption-desorption parameter (k_{ads} , k_{des}) vary more pronouncedly over the years than transformation ones ($DT_{50,w}$, $DT_{50,s}$, and $DT_{50,p}$) (Tables A.2 & A.3). In order to evaluate this variability, we ran the model using a generic set of parameters (Table 3), which is the mean value of the annual-calibrated parameters (Tables A.2 & A.3) and estimated the performance criteria (Table 3). Additionally, a graphical comparison between the simulations using the calibrated parameters and the non-transformed observations is provided (Fig.3).

Table 2: The mean value of the annual-calibrated parameters, and the PPDB values of transformation half-lives, i.e., ($DT_{50,w}$, $DT_{50,s}$, and $DT_{50,p}$). The physicochemical properties were extracted from the PPDB or other pesticide databases if not available.

Pesticides	Calibrated					PPDB			PPDB/Literature	
	$DT_{50,w}$	$DT_{50,s}$	$DT_{50,p}$	k_{ads}	k_{des}	$DT_{50,w}$	$DT_{50,s}$	$DT_{50,p}$	K_{oc}	$\log K_{ow}$
Bentazon	5	100	3	0.15	0.01	80	716	4	55	2.34
Boscalid	500	500	stable	0.63	0	5	545	stable	772	3
Chlorotoluron	44	300	30	0.42	0	44	308	30	400	2.5
Diflufenican	200	175	133	0.51	0	200 ²	175	stable	550	4.2
Mesotrione	5.3	5.2	89	0.69	0.05	5.3	5.2	89	122	0.11
S-metolachlor	1.5	43	146	0.07	0.01	9	43	146	120	2.9
Quinmerac	3.84	180	66	0.43	0.02	88	179	66	86	2.7

Table 3: Statistical comparison of simulations and daily observations of pesticide fluxes. The left part of the table lists the KGE, NSE, and NRMSE values using an inter-annual set of parameters, i.e., the mean of the annual-calibrated parameter values, and the right part is for the annual calibration

Pesticides	Inter-annual calibration			Annual calibration		
	KGE	NSE	NRMSE	KGE	NSE	NRMSE
Bentazon	0.74	0.79	0.07	0.75	0.79	0.07
Boscalid	0.44	0.64	0.06	0.68	0.68	0.06
Chlorotoluron	0.74	0.87	0.01	0.83	0.82	0.05
Diflufenican	0.76	0.78	0.07	0.74	0.73	0.05
Mesotrione	0.63	0.93	0.03	0.69	0.87	0.04
S-metolachlor	0.58	0.76	0.04	0.58	0.75	0.05
Quinmerac	0.54	0.84	0.04	0.65	0.86	0.04

High KGE (>0.5) and NSE (>0.6) values of the model outputs were observed when using the inter-annual set of parameters for all pesticides (Table 3). Boscalid made the exception with a KGE of 0.44. Given that the annual calibration was designed to find a proper set of parameters for each period (Tables A.2 & A.3), the performance was expected to decrease when running the model with a single set of parameters independently of the period (Table 2). Nonetheless, the criterion values reflect in aggregate a good model performance, i.e., NSE >0.35 and KGE >0.5, except for boscalid, which indicates a not satisfactory performance according to the commonly used thresholds (Knoben et al., 2019; Moriasi et al., 2015; Towner et al., 2019).

² The biotransformation half-life in water of diflufenican was not available in the PPDB so it was extracted from EFSA (2008). Conclusion regarding the peer review of the pesticide risk assessment of the active substance diflufenican. *EFSA Journal* 6, 122r.

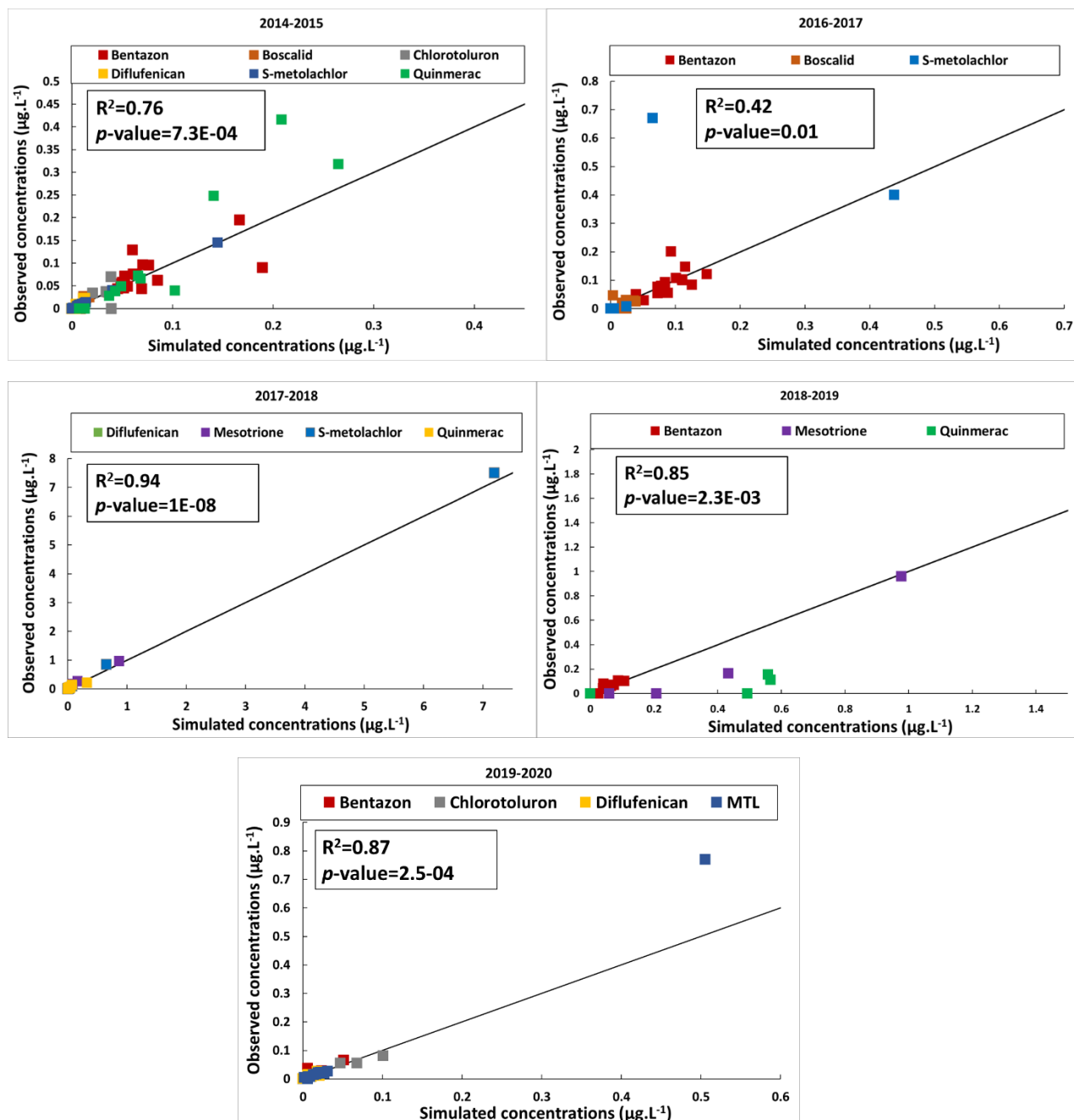


Figure 3: Graphical comparison of the bi-monthly observations (y-axis) and simulations (x-axis) of all pesticide outlet concentrations ($\mu\text{g.L}^{-1}$) and periods combined, using the inter-annual calibration. Each color points out a specific pesticide. The black line in the middle refers to simulations equal to observations ($Y=X$). R^2 is the R-squared correlation coefficient between the observations and simulations. $p\text{-value}^3$ is the $p\text{-value}$ of the regression test.

Using the inter-annual set of parameters results in a good fit between the simulations and the non-transformed observations of pesticide concentrations (Fig.3). The R^2 values were >0.7 ($p\text{-values} < 0.05$), indicating a strong correlation between the observations and simulations, except during 2016-2017 ($R^2=0.41$). The s-metolachlor simulated concentration ($0.5\mu\text{g.L}^{-1}$) was underestimated compared to the observations ($0.77\mu\text{g.L}^{-1}$) during 2019-2020. The underestimation was more accentuated during 2016-2017 when the simulated concentration of s-metolachlor ($0.06\mu\text{g.L}^{-1}$) was ten times lower than the observations ($0.67\mu\text{g.L}^{-1}$). The poor

³ A $p\text{-value} < 0.05$ indicates that the correlation between the observations and simulations is statistically significant.

performance of the model evidenced by the low KGE value of boscalid is also noticed by the overestimation of the exported mass during 2016-2017 and the pronounced underestimation during 2014-2015 (Fig.A.6). On average, the relative error of boscalid discharge simulations is 36% while it is <10% for other pesticides. The *p*-values of the *t*-test were >0.05, reflecting that the null hypothesis cannot be rejected (Table A.4). Hence, there is no significant difference between the observed and simulated pesticide concentration for all periods. The high R^2 values indicate a strong correlation between the observed and simulated pesticide concentration, except for 2016-2017, manifesting a moderate correlation—the *p*-values of the regression analysis evidence the statistical significance of these correlations (Table A.4).

Altogether, the graphical and statistical comparison of the observations and the simulations using the inter-annual set of parameters reflect a good model performance for all pesticides except for boscalid. After the quantitative evaluation of the model, the next section will describe the mass budget of pesticides within the AP and the contribution of each process to pesticide dissipation.

3.3 Pesticide mass budget

One of the PESTIPOND model's major aims is to quantify each process's contribution to the fate of pesticides. Accordingly, after running the model with the mean set of parameters, the mass budget of pesticides was assessed to illustrate the mass distribution in the pond and the contribution of each process to pesticide dissipation. Table A.5 summarizes the mass budget for all the pesticides and periods of the survey. Note that the PESTIPOND model checks whether the mass balances tally during the calculations. The mean mass balance error of the set of pesticides and periods is <1 % showing that the model conserves the mass properly.

For succinctness, only mean values of the mass partition in the AP at the end of each period will be discussed in the following (Fig.4). Note that the transformation in water includes the biotransformation, photolysis, hydrolysis, and volatilization in the water column.

Overall, most intercepted pesticides are discharged from the pond with a mean out flux of 72%, followed by the mass remaining in the active sediment layer with a mean proportion of 12%, which leaves almost 2% pesticides in the water column. Therefore, the mean dissipated mass between the inlet and outlet of the AP accounts for 14% of the total intercepted mass.

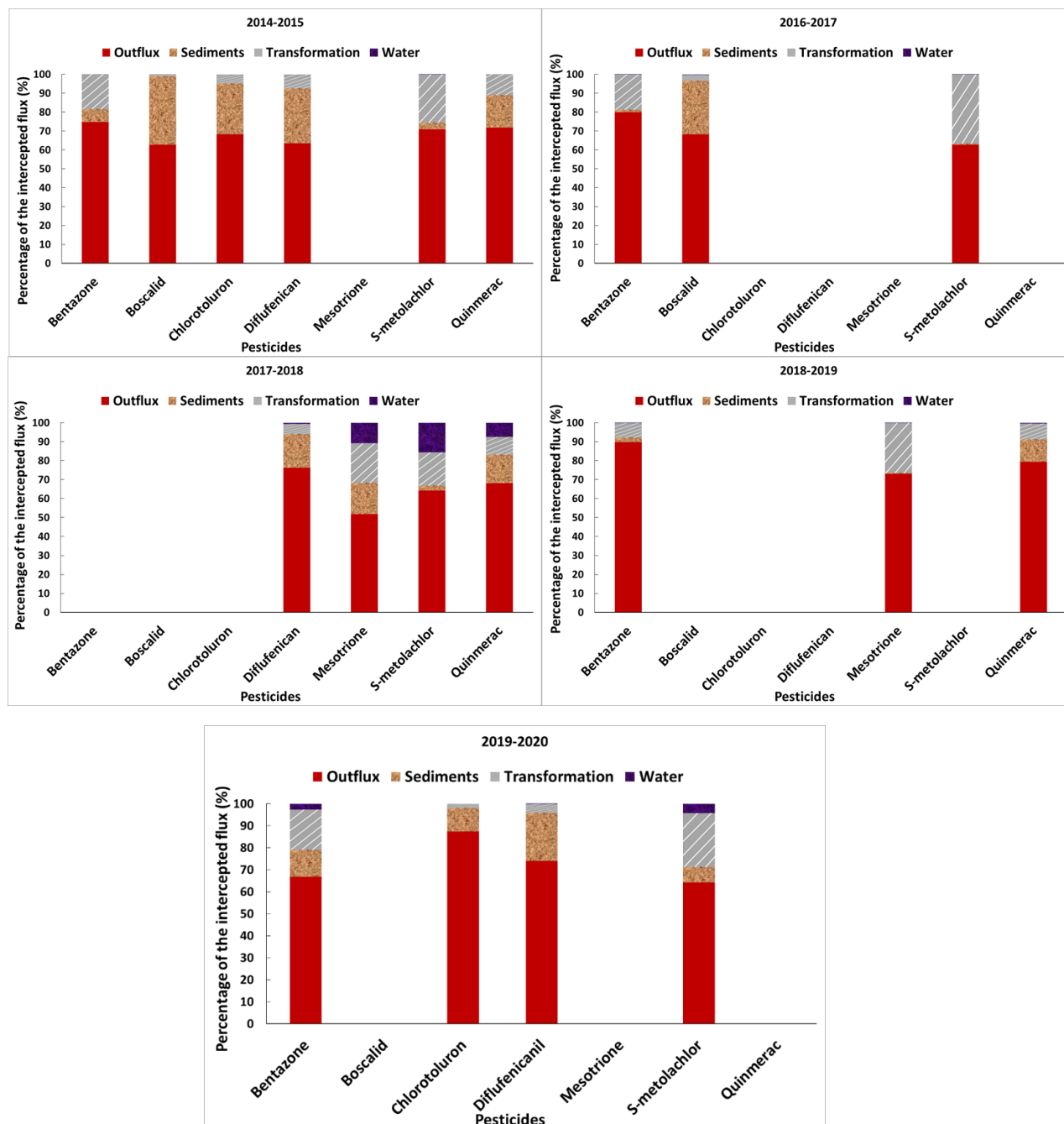
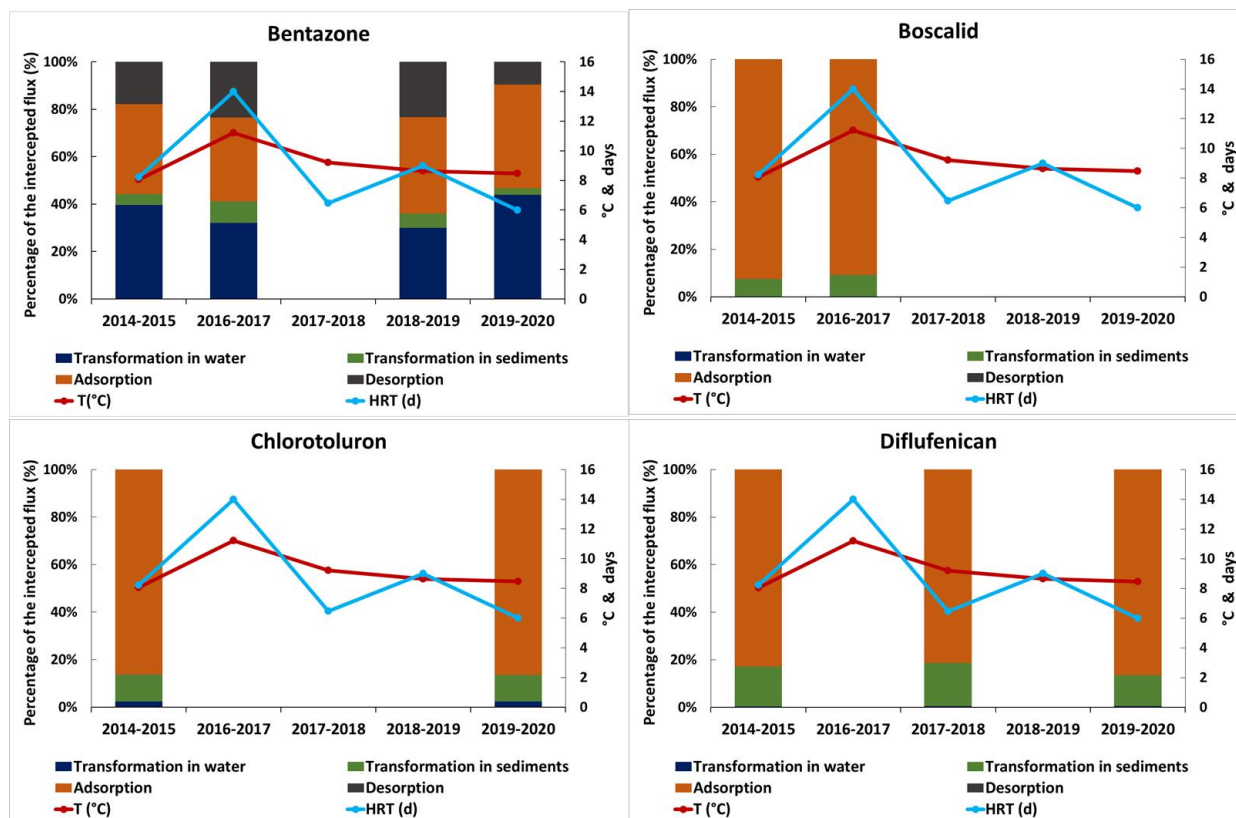


Figure 4: Graphical representation of the proportion of pesticide masses to the total input mass.

On average, boscalid, mesotrione, and quinmerac had the highest adsorption (Fig.4), which covers 35%, 36%, and 35% of the total input mass, respectively (Table A.5). Diflufenican, chlorotoluron, and bentazon come after with adsorption of 28%, 21%, and 14%, respectively. S-metolachlor had the lower adsorption (6%) but a significant transformation in water (24%), which is mostly due to biotransformation (23%), leaving only 1% to the other transformation processes (photolysis, hydrolysis, and volatilization). A significant transformation in the water column was also noted for bentazon (14%), which is mainly partitioned between photolysis (9%) and biotransformation (5%). On the other hand, biotransformation at the water-sediment interface had an important contribution to pesticide dissipation. For instance, 18% of the mesotrione intercepted mass was biodegraded on average in the active sediment layer.

Moreover, during 2014-2015, boscalid, chlorotoluron, and diflufenican were more transformed in the sediments than in water. The transformation in water and desorption rates for the same three pesticides are negligible (<1%). Conversely, the quinmerac desorption covers 20% of the inlet mass, followed by mesotrione (10%) and bentazon (7%). The photolysis contribution to dissipation was negligible for all pesticides except for the bentazon (8%).

Temperature was the highest during 2016-2017, which overlapped with the highest, desorption and transformation of bentazon at the water-sediment interface. The same period exhibited the highest HRT.



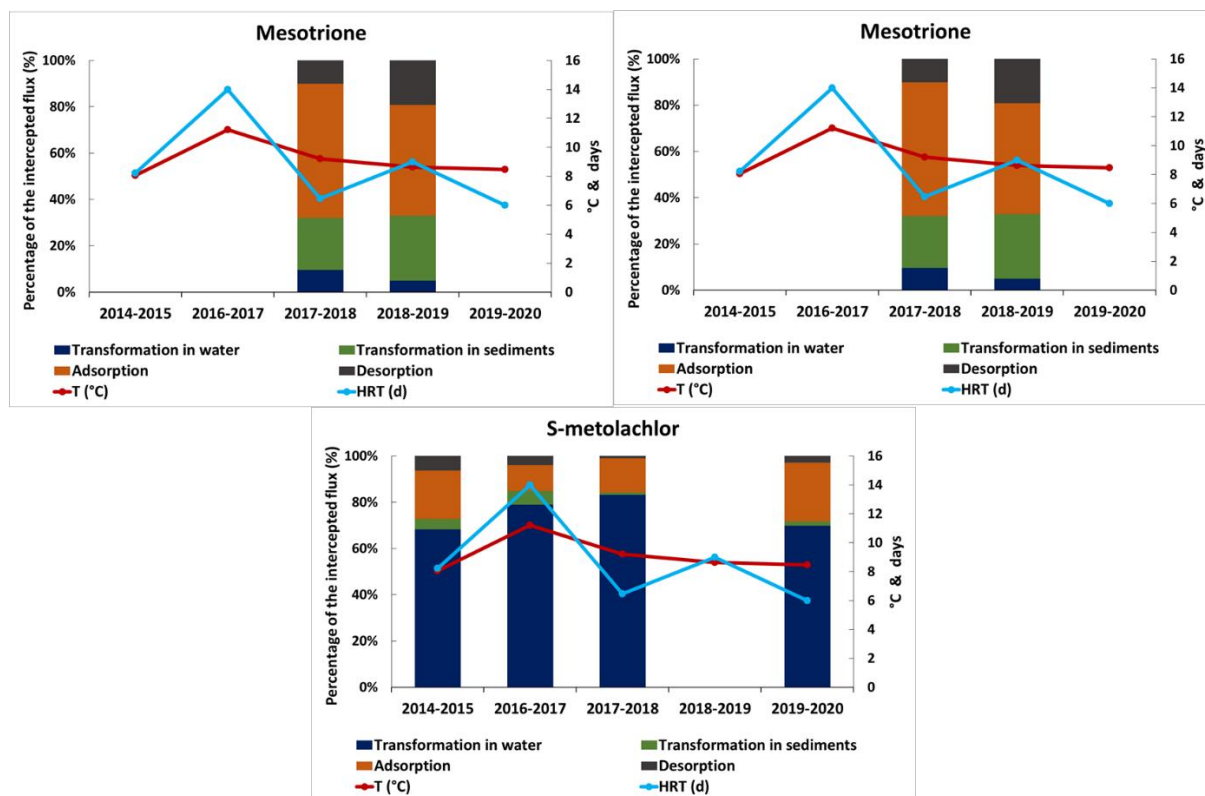


Figure 5: Graphical representation of the percentage of each process to the total mass intercepted by the pond and, the average temperature T (°C) and HRT (d) of each period.

3.4 Model extrapolation: Efficiency abacus

For further exploitation of the model outputs, PESTIPOND was run with the inter-annual parameter set described in section 3.3 and the same inputs presented in Section 2.3 but using different AP sizes in ascending order, equivalent to higher nominal HRT. For each simulation assigned to a specific AP area A (and HRT), the mean pesticide dissipation efficiency was computed (Eq.1). For the different simulations, only the AP area was modified, and the rest of input data were kept the same (e.g., the water flow rates, water depth, and temperature).

Note that a mean efficiency, including all pesticides, is computed for each period, and then a mean value for all periods is deduced (Fig.6, Table. A.7).. For this extrapolation study, boscalid was excluded because it yielded poor model performance (section 3.2).

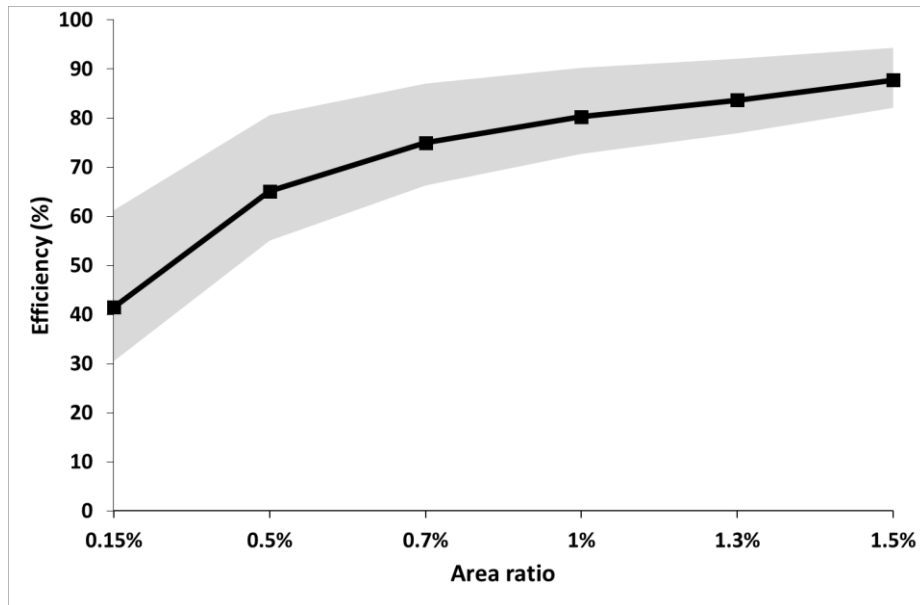


Figure 6: The mean efficiency of the Rampillon AP to dissipate pesticides from the inlet to the outlet according to the different sizes of the pond. The x-axis represents the percentage (%) of the area occupied by the AP in the total catchment area (355ha). The y-axis corresponds to the mean efficiency of the studied periods. The upper and lower grey areas refer to the discrepancy between the mean and the maximum and minimum efficiencies, respectively.

For the actual Rampillon area (5270m²), which covers 0.15% of the drained catchment area (355ha), the mean AP efficiency is 40% for all pesticides combined. By increasing the surface area by 10 000 m², the HRT is tripled, and the efficiency rises sharply to 63%. From an area that covers 0.7% of the watershed, the efficiency increases less steeply and attains about 82% (Fig.6).

An annual variation of the simulated pond efficiency independently of the area was noticed (Fig.A.8). However, the variation degree decreased with increasing pond areas, as well as the efficiency itself, as observed in Fig.6. For the actual AP size (i.e., 0.15% of the catchment area), the efficiency doubled from 2014-2015 (30%) to 2016-2017 (62%). Afterward, the dissipation potential of the pond decreased sharply to 36% during 2017-2018 and remained around 38% for the following years. Similar behavior will be noticed in the pond's efficiency if the surface increases to 0.5%-0.7% of the catchment area, with higher minimum and (55%-66%) and maximum values (80%-87%), respectively. For a ratio of 0.15%-0.7%, the mean pond dissipation is 17% lower than the mean maximum and 10% higher than the minimum. Conversely, once the AP area covers >1% of the catchment, the discrepancy between the mean efficiencies and the minimum and maximum values decreases to ~8% and ~6%, respectively (Fig.6).

In addition, similar extrapolation was performed on different temperatures representing a geographical temperature gradient (Fig.A.9). Pesticide dissipation increases linearly according to ascending temperature. On average, the current temperature of the surveyed periods is 9°C, which results in a 40% efficiency of the Rampillon AP.. In aggregate, a temperature rise of 5°C will boost the mean efficiency by 4%. Overheating the current temperature by 10°C will improve the mean dissipation of pesticides by almost 13 %. A temperature rise of 5°C will result in a maximal mean efficiency of 67%, compared to the actual maximal dissipation rate (61%). A lower variation is noticed in the minimum pond efficiency with ascending temperatures. On average, the actual minimal dissipation rate of the AP is 30%, which is also

expected to rise by 4% due to a temperature increment of 5°C. On the other hand, reducing the temperature by -5°C can decrease the actual efficiency by 2%.

4 Discussion

4.1 Conceptual model

PESTIPOND is a time-dependent model (daily-step) developed to predict the fate of pesticides at the ponds' scale before being transferred to the water resources of the agricultural catchment. The model is designed to be implemented in a landscape-modeling tool (e.g., SWAT (Neitsch et al., 2011)) to predict pesticide behavior at the catchment scale. PESTIPOND can be integrated into landscape modeling by replacing the equations of the pesticide fate sub-model with PESTIPOND's formulations. Otherwise, the pesticide concentrations simulated by PESTIPOND could be directly implemented as simulated data in landscape models. The PESTIPOND modeling approach is built upon the mass balance of pesticides in the two main compartments of AP, i.e., the water column and the active sediment layer, also designated as the water-sediment interface, while considering the key physicochemical processes behind pesticide behavior. PESTIPOND requires hydro-climatic input data (i.e., rainfall, PET, temperature, inflow, and outflow rates) and monitoring data of the intercepted pesticides (inlet concentrations).

The originality of the model lies in integrating and exploring the key physicochemical processes to predict the export of pesticides from AP contrarily to black-box models using a single generic decay coefficient. Besides, PESTIPOND uses the simplest form of mathematical formulations when compared to more complex and computationally costly environmental fate models such as TOXSWA and AGRO-2014 (Adriaanse, 1996; Gobas et al., 2018). Contrarily to other pesticide fate models (i.e., the pond/lake module of SWAT (Neitsch et al., 2011)), PESTIPOND integrates the effect of temperature and HRT as they are widely recognized as governing factors of pesticide behavior in AP. Each temperature-dependent process coefficient is adjusted to the actual site temperature. Plus, the processes are integrated into the model by kinetics; thus, the more extended the HRT, the longer the process will have time to dissipate the molecule. In contrast to SWAT, PESTIPOND integrates desorption, a considerable process for mobile and hydrophilic pesticides, as underlined by the SA and mass budget results discussed afterward.

4.2 Sensitivity analysis

A global sensitivity analysis was performed and documented in (Bahi et al., 2023, submitted). SA outcomes evidenced the insensitivity of the PESTIPOND model to hydrolysis and volatilization processes. By contrast, adsorption and desorption showed the most significant influence on pesticide behavior independently of their molecular properties. Similar SA assumptions were made by Boulange et al. (2012) and Desmarteau and Ritter (2014) for other environmental fate models. In addition, SA evidenced that the biotransformation at the water-sediment interface is more effective on hydrophobic and lowly mobile pesticides, while biotransformation in water is more effective on hydrophilic and highly mobile pesticides. The variation of the AP efficiency with time (Fig.A. 7) can be translated by the seasonal change of the impact of processes on pesticide fate. This observation fortifies the SA assumption outlining that (1) the sensitivity of hydrophilic pesticides to sorption and transformation processes varies with time according to the hydraulic conditions of the AP and (2) that temperature has a major effect on the set of processes, particularly enhancing pesticide transformation. Afterward, the model was calibrated and validated using monitoring data of 7 pesticides with contrasted

properties (i.e., hydrophobicity and mobility) during five periods. PESTIPOND performance was graphically and statistically evaluated.

4.3 Model performance

For the model performance assessment, we adopted the following strategy. The performance of PESTIPOND was first (i) evaluated using an annual calibration (i.e., a set of parameters proper to each year (Tables A.2 & A.3) and then (ii) a generic set of parameters for all years (i.e., the mean value of the annual-calibrated parameters (Table 2). Since the daily observations of pesticide concentrations are not available, transformed observation data was created from bi-monthly monitoring to illustrate pesticide dynamics closely. Therefore, the model performance was assessed for both transformed and non-transformed observations for each step (i) and (ii).

Firstly, the results of steps (i) and (ii) of the performance assessment (section 5.2) proffered graphical (Fig.2, Fig.3) and statistical (Tables 3 & A.4) agreements between simulations and observations except for boscalid according to non-transformed observations. Given the half-lives of boscalid reported in the literature (PPDB), it is biodegradable in water. Whereas boscalid was stable based on the observations in the Rampillon AP (Fig A.5), which means that the conditions in which the PPDB half-lives were estimated may be different from those of an AP.

Lower KGE and NSE values were noted for step (ii) compared to (i). The drop in the performance (ii) was expected since the annual calibration uses an adapted set of parameters for each year (Tables A.2 & A.3), whilst a single set of parameters was used for all years combined in the performance assessment (i) (Table 3).

Secondly, a lower KGE was noticed for all pesticides compared to the NSE values. The difference between the KGE and NSE values may originate from the definition of the KGE (Eq.3) based on the mean difference between simulations and observations, which puts more weight on extreme values. Alternatively, the NSE (Eq.4) estimates the discrepancy between observations and simulations evenly during the whole period. Given that a spike following their application in the agricultural plots characterizes all the pesticide chronicles, it is anticipated that the KGE will have lower values than the NSE. Notwithstanding, it is recommended to evaluate model performance with more than one criterion (NSE), thus using the KGE and NRMSE. Based on commonly used thresholds (Knoben et al., 2019; Moriasi et al., 2015; Towner et al., 2019), the KGE and NSE values indicate a “good” model performance, except boscalid, for which the model performance is considered as “not satisfactory” according to both transformed and non-transformed observations. The low model performance on boscalid is also portrayed by a significant discrepancy between the observed and simulated exported mass and outlet concentration during 2014-2015 (Fig.A.6). Furthermore, boscalid simulations induce a model relative error (36%) higher than other pesticides (<10%). Moreover, the average NRMSE translates to a slight discrepancy between the observed concentrations and simulations for the other pesticides.

Note that using the transformed observations (daily) evaluates the model's ability to simulate pesticide dynamics. The non-transformed observations (bi-monthly) assess the model's capacity to predict the exported fluxes and concentrations of pesticides from the AP. Therefore, based on the graphical and statistical comparisons between the model outputs and both the transformed and non-transformed observations while using a single set of parameters (inter-

annual), we assume that the PESTIPOND model is robust and able to predict the dynamics and exported fluxes and concentrations of pesticides, except for boscalid, at the AP scale.

4.4 Hierarchization of pesticide dissipation processes

To further explore the model outcomes and confirm the SA assumptions, we closely analyzed the mass budget of pesticides in the AP. We quantified the contribution of each process to pesticide fate. The quantification of the mass partition of pesticides revealed that most of the intercepted mass is discharged from the pond for a mean residence time of 16 days and 9 °C temperature. The remaining mass is dissipated or stored in sediments and in the water column. The pesticides that were mostly stored in the sediment layer are boscalid (K_{oc} (L.kg⁻¹) = 772, log K_{ow} =3), chlorotoluron (K_{oc} (L.kg⁻¹) = 400, log K_{ow} =2.5), and diflufenican (K_{oc} (L.kg⁻¹) = 550, log K_{ow} =4.2). According to their K_{oc} and K_{ow} , these three molecules are hydrophobic (log $K_{ow} \geq 3$) and lowly mobile ($K_{oc} > 500$) (Lewis et al., 2016). Therefore, they are likely to be adsorbed on sediments, which agrees with the mass budget results (Fig.5). Alternatively, the pesticides manifesting a higher presence in water are mesotrione (K_{oc} (L.kg⁻¹) = 122, log K_{ow} =0.11), s-metolachlor (K_{oc} (L.kg⁻¹) = 120, log K_{ow} =2.9), bentazon (K_{oc} (L.kg⁻¹) = 55, log K_{ow} =2.34), and quinmerac (K_{oc} (L.kg⁻¹) = 86, log K_{ow} =2.7), which are hydrophilic and highly mobile (Lewis et al., 2016). The results purport that PESTIPOND simulates a pesticide behavior in agreement with the one expected based on their properties.

The PESTIPOND model was initially built to hierarchize the processes behind pesticide dissipation. This hierarchization is useful for identifying the key elements to be managed in order to optimize the environmental efficiency of ponds. Thus, the mass attributed to each process was quantified and confronted with temperature and HRT. For all pesticides, adsorption is the most significant process in pesticide behavior, except for s-metolachlor (4), which was more distinguished by the transformation in the water column. By relating this result to the hydrophilic and mobile properties of the pesticide, it is expected that s-metolachlor undergoes limited adsorption, which increases its bioavailability for transformation in the water column than the sediment layer. A similar observation was made for s-metolachlor by (Droz et al., 2021) based on laboratory experiments. By contrast, more significant adsorption was detected for the hydrophobic boscalid, chlorotoluron, and diflufenican (Fig.5), followed by a transformation in the sediment layer. In fact, the significant adsorption of hydrophobic pesticides was heavily evidenced in the literature (Hand et al., 2001; Tang et al., 2017; Vagi and Petsas, 2022) based on their high affinity to the organic carbon of sediments and hydrophobicity translated by a high K_{oc} and log K_{ow} , respectively. Boscalid, chlorotoluron, and diflufenican are more likely to be adsorbed on sediments and thus are more bioavailable for biotransformation at the water-sediment layer, contrarily to more hydrophilic and mobile pesticides. For instance, bentazon, s-metolachlor, and quinmerac being hydrophilic and highly mobile, are more likely to be transformed in water (Table A.6). This result underlines the link between adsorption and pesticide bioavailability for biotransformation as suggested by previous experimental studies (Ahmad et al., 2004; Budd et al., 2011; Chaumet et al., 2021; Lee et al., 2004; Mulligan et al., 2016). The low log K_{ow} (<3) of bentazon, mesotrione, and quinmerac indicate that they are likely to be re-mobilized from the sediment, which was reflected by the mass budget detecting a desorption flux for all monitoring periods. For hydrophilic and highly mobile pesticides, desorption covered a non-negligible part of the intercepted mass.

On average, for all pesticides and periods combined, adsorption covers 22% of the input mass, followed by 10% for biotransformation in water and desorption with 6%, leaving 5% for biotransformation and the water-sediment interface. Photolysis covers a negligible part of the total transformation in water ($< 1\%$), except for bentazon ($\approx 8\%$). However, when looking at pesticides separately, hydrophobic and lowly mobile pesticides had higher biotransformation at the water-sediment interface than in the water. The mass budget results support the significance of adsorption, desorption, and biotransformation in the water for hydrophilic and mobile pesticides. Alternatively, biotransformation at the water-sediment interface is more pronounced and, desorption is limited for hydrophobic and lowly mobile pesticides.

SA results contended that adsorption is the most influencing process of pesticide behavior, fortifying the mass budget results showing that an important fraction of the intercepted mass was adsorbed for most pesticides. The mass budget also exhibited a higher transformation in water and desorption effect on hydrophilic and mobile pesticides, explaining why these types of molecules were more sensitive to processes occurring in the water column. Conversely, hydrophobic and lowly mobile pesticides were distinguished by higher adsorption and transformation in the active sediment layer, which is in line with the SA outcomes displaying a higher sensitivity to processes occurring at the water-sediment interface for this kind of pesticides. Combining the model results and SA outcomes, we assume that adsorption-desorption and biotransformation are major processes behind pesticide fate. Hydrophobic and lowly mobile pesticides are more likely to be biotransformed in the active sediment layer than in water. At last, volatilization and hydrolysis have a negligible contribution to pesticide dissipation.

4.5 Dissipation efficiency and pond properties

In addition, the PESTIPOND model enables the assessment of the link between pesticide dissipation and pond properties (i.e., temperature and HRT). The mass budget results (Fig.4) highlighted a higher transformation of bentazon, boscalid, and s-metolachlor 2016-2017, characterized by the highest mean temperature (12°C) and HRT (28 days). Also, bentazon, diflufenican, and s-metolachlor underwent higher adsorption during 2019-2020, having a higher HRT (27 days). The same pesticide had a lower transformation during 2018-2019, characterized by a lower mean temperature (8°C). Moreover, the desorption of bentazon and mesotrione was more significant during 2018-2019, when the HRT was only 8 days.

These results support the link between temperature, HRT, and pesticide behavior. Higher temperatures enhance the microbial activity behind the biotransformation and are accompanied by important solar radiations, which favors photolysis (Kaur and Vishnu, 2022; Law et al., 2014; Motoki et al., 2020; Rani and Sud, 2015). Therefore, significant pesticide transformation was noticed during periods of high temperature. In addition, higher HRT provides a longer time for pesticides to be adsorbed and transformed. Similarly, for some pesticides higher desorption was noted during low-HRT periods while it was the opposite for other pesticides. This result suggests that no direct link between desorption and HRT was noticed.

The link between temperature, HRT, and pesticide dissipation raises concerns about the impact of pesticides' application period. For instance, except for chlorotoluron, the set of pesticides is applied in spring, which tends to have significant rainfall events. Therefore, during spring, pesticides are more likely to be intercepted by the AP due to runoff following rainfall events and thus be dissipated by the synergy of the above-described processes. Moreover, spring-

applied pesticides are more susceptible to transformation as the temperatures rise. Although this is also the case for summer-applied pesticides, it is unlikely that these chemicals will get to the pond due to limited rainfall events. Alternatively, pesticides applied during winter and autumn, such as chlorotoluron, even though intercepted by the AP, their transformation is less expected due to the weak microbial activity associated with cold temperatures. This assumption could explain the mass budget result illustrating a lower transformation of chlorotoluron, which is applied during autumn and winter in Rampillon. By contrast, spring and summer-applied pesticides (i.e., bentazon, mesotrione, and s-metolachlor) were more favorable to transformation in the water column (Table A. 6). The model extrapolation results evidenced that a temperature rise of 10°C will increase the mean dissipation potential of the AP by 13% (Fig.A.9). In comparison, a temperature drop of 5°C decreases the efficient by only 2%. These results provide insight into the geographical variation of AP efficiencies between warm and cold areas.

Besides low temperatures, winter and autumn-applied pesticides face strong flows that reduce their residence time in the pond to undergo the different dissipation processes. Therefore, to remediate this issue, the surface area of the AP can be enlarged to increase the HRT and, thus the residence time of pesticides. Accordingly, an estimation of the AP efficiencies according to ascending surface areas (Fig.6) was performed. The results showed that once the AP covers >1% of the drained catchment area, the dissipation of pesticides reaches 84%, which is almost twice and a half of the actual efficiency of the Rampillon AP. [Tournebize et al. \(2012\)](#) reported that, based on a literature review of AP performances, scientists suggested allocating 1% of the catchment area to the pond. However, farmers rejected this proposal for different reasons (land occupation, cost, operational labor cost, and maintenance). Consequently, the farmers suggested a 0.15% area for the AP to meet their requirements or acceptability, which was expected to be a less efficient remediation solution for pesticide transfer. The PESTIPOND simulations, predicting a significantly higher efficiency of the AP if it covers 1% of the catchment, supported this expectation. In addition, the extrapolation results evidenced that the HRT has a significantly higher impact on the AP efficiency when compared to the temperature rise. This assertion was expected since the HRT drives the efficiency of all processes, namely adsorption, desorption, and transformation, while temperature only influences transformation processes. This assumption is supported by the mass budget results, indicating a higher transformation of pesticides during high-HRT periods (2016-2017) even though the temperature is low. In addition, adsorption is a major dissipation process occurring mainly at the water-sediment interface. Hence, increasing the HRT by increasing the AP area is equivalent to increasing the water-sediment interface where pesticide retention occurs. This explains the higher efficiency in larger ponds and the major role of the water-interface sediment in pesticide dissipation.

From another viewpoint, adsorption can be a concern over the long term as it accumulates pesticides in the sediment. However, recent in-situ measurements of pesticide concentrations in the Rampillon AP sediments showed that after ten years, only a few amounts of pesticides were accumulated (<7ng.g⁻¹). Moreover, another in-situ experiment was performed in mesocosms, evidenced that bentazon was the only pesticide sensitive to light, which supports the model result indicating a significant photolysis of the molecule in question.

4.6 Calibrated parameters and pesticide properties

The parameter set used for this model validation was compared to literature values. Due to the non-availability of adsorption-desorption parameters, k_{ads} and k_{des} were calibrated. The obtained values were in the order of magnitude of similar studies' calibrated parameters (Comoretto et al., 2008; Nakano et al., 2004; Watanabe et al., 2006; Yoshida and Nakano, 2000). In addition, a strong correlation ($R^2=0.9$) between k_{ads} and K_{oc} was noticed, except for s-metolachlor (Fig.A.7). A first correlation equation was defined for mobile pesticides ($K_{oc} < 120 \text{ L.kg}^{-1}$) and a second one for lowly mobile pesticides ($K_{oc} > 300 \text{ L.kg}^{-1}$). For mobile pesticides, the desorption parameter can be deduced from the adsorption kinetic and set to zero for lowly mobile molecules. Transformation parameters ($DT_{50,w}$, $DT_{50,s}$, and $DT_{50,p}$) were extracted from the PPDB (Lewis et al., 2016), and some were calibrated to improve the model performance (Table 2). The calibrated parameters were $DT_{50,w}$ and $DT_{50,s}$ for 4 pesticides out of 7. Globally, the calibrated half-lives were shorter than the PPDB values. In water, the dissipation was, on average, 75, 7, and 80 days faster for bentazon, s-metolachlor, and quinmerac, respectively, than in the laboratory (i.e., where the PPDB values are estimated). In the water-sediment interface, the dissipation was, on average, 600 and 8 days faster for bentazon and chlorotoluron, respectively. This result indicates a faster dissipation under field conditions than in laboratory experiments. The same assumption was made by Bahi et al. (2023b), suggesting that pesticides face a single process in laboratory experiments (PPDB). Contrastingly, pesticides undergo a synergy of on-site processes that enhance their dissipation owing to a shorter half-life. Boscalid was the only pesticide having a calibrated $DT_{50,w}$ (500 days), a hundred times longer than the PPDB value (5 days), which may explain the low model performance according to this molecule. However, other sources substantiate the belief that boscalid is stable in water and sediments and is rather adsorbed on sediments (Keith and Walker, 1992; Mergia et al., 2022), assisting the mass budget results (Fig.4).

4.7 PESTIPOND limitations

The strong foundation on which this model is built is represented by the numerous results of pesticides with contrasting properties and application periods. However, the limitations of PESTIPOND should be recognized. First, the assumption of a completely mixed reactor is not always the case in APs, specifically those representing heterogeneities (i.e., significant vegetation cover, dikes, and dead zones). Therefore, the PESTIPOND model could be complemented if coupled with hydraulic-based models, such as 3D or 2D models (Lemaire et al. (2022), *under review*). 3D computational fluid dynamics models incorporate relevant pond compartments (plant/water and sediment/plant interfaces). However, these compartments may require excessive computation time (Tsavdaris et al., 2013). Therefore, 2D models are a better alternative, as they are less computationally costly and include explicitly the vegetation patches to estimate the water pathways and their transit times in ponds (Imfeld et al., 2021; Silva and Ginzburg, 2016). Secondly, considering microbial communities' acclimation and dynamics will undoubtedly improve the model's performance. The model prediction could also be expounded by considering the fate of transformation products. Additionally, if the model integrates the dynamics of organic carbon content, the adsorption-desorption effect would be better expounded.

The model was validated for bi-monthly observations of pesticides. Yet, the accuracy of PESTIPOND validation can be ameliorated if daily observations of pesticides were available. Notwithstanding, the model is robust and simulates a pesticide behavior close to observations

and the one expected based on molecular properties. In addition, PESTIPOND is a readily configurable model since the transformation parameters can be inspired from literature (PPDB) and adsorption-desorption parameters deduced from the pesticide property K_{oc} . Furthermore, the originality of PESTIPOND lies in the ability to predict pesticide partition in AP and quantify the contribution of each physicochemical process to their overall behavior while integrating temperature and HRT effects.

5 Conclusion

PESTIPOND is a process-based model developed to predict the fate of pesticides in APs. The model is designed to be integrated into landscape agro-hydrological modeling tools to extrapolate the prediction to the catchment scale.

The key assumptions to be drawn from this study are (i) that adsorption-desorption and transformation are governing processes in pesticide fate. (ii) Hydrophobic and lowly mobile pesticides are more likely to be transformed at the water-sediment interface. Although the fate of the transformation products is still unknown, the exported amount of mother pesticide molecules will be dissipated before reaching natural water resources. (iii) Hydrophilic pesticides, despite being less retained in APs, can be subjected to transformation in the water column, especially during summer and spring, when temperature arises. A higher HRT will increase the dissipation probability for both hydrophilic and hydrophobic pesticides in the water column. Longer HRT provides more time for pesticides to be adsorbed and transformed within the AP. Accordingly, the PESTIPOND model predicted that the actual efficiency of the AP covering 0.15% of the drained catchment would double if the pond's surface area covered at least 1% of the catchment. By contrast, the model's predictions evidenced that a temperature rise of 10°C will increase the dissipation of pesticides by only 8%. It is noteworthy that a temperature rise entails a more significant transformation and hence more transformation products. However, the model does not consider these latter, which can be addressed later by adding a transformation products compartment to predict its fate in APs.

Given that, we assume that PESTIPOND provides key elements that are useful to design and manage ponds with optimal efficiency. Hence, these ponds can be complementary solutions to pesticide use regulation to reduce the transfer of agricultural contamination into the environment. PESTIPOND can be implemented afterward in landscape modeling tools to extrapolate the prediction of pesticide behavior from the pond scale to the catchment scale.

6 Appendix

6.1 Properties of the Rampillon AP

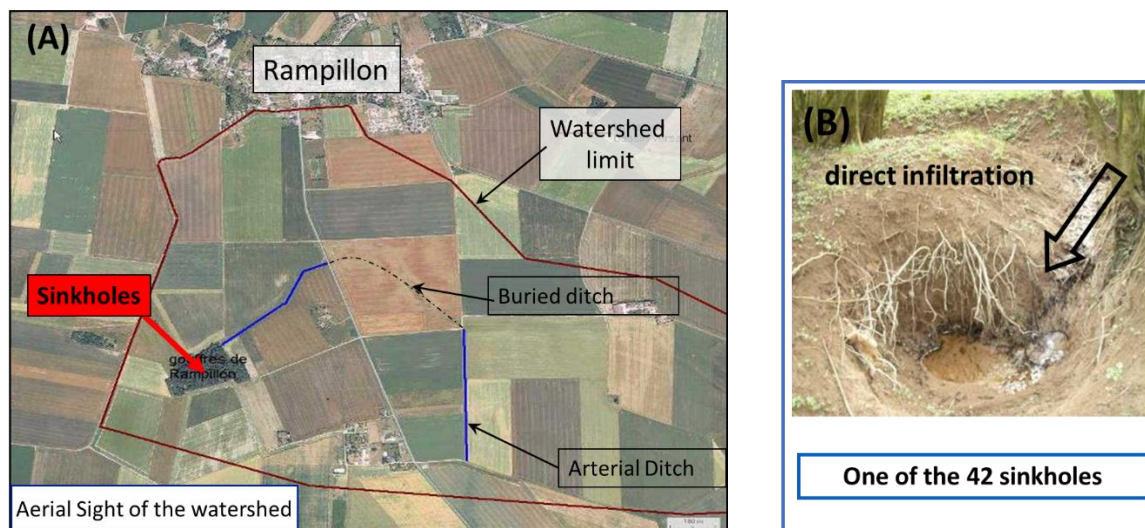


Figure A.1: Aerial sight of the Rampillon watershed (355 ha) (A). The watershed comprises two arterial ditches (blue lines) and a buried ditch (dashed line). The red arrow points toward sinkholes. Fig.A.1 (B) displays one of the 42 sinkholes contained in the watershed.

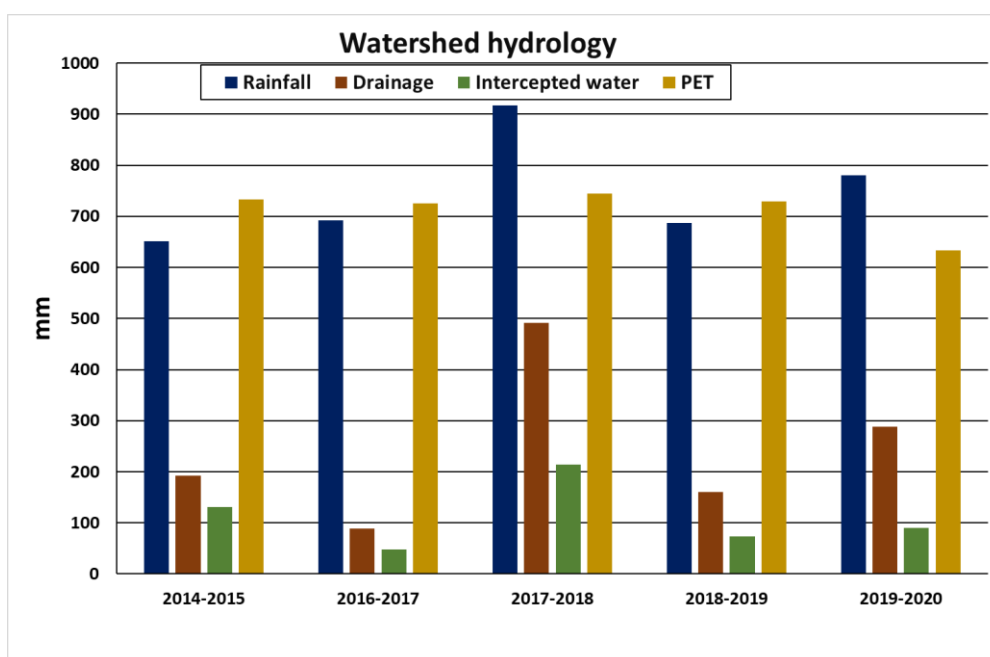
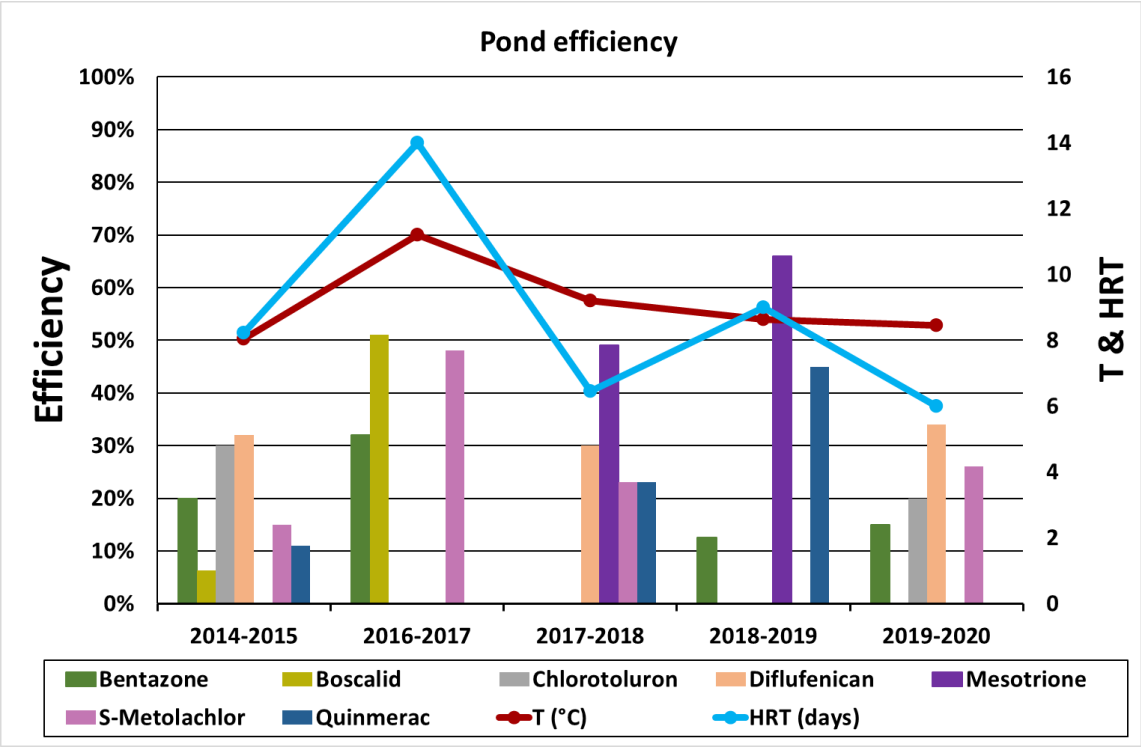


Figure A.2: Summary of hydrological inputs of the 355-ha watershed where the Rampillon AP is implemented. The blue bars represent the local rainfall, the brown bars represent the drained water in the watershed, the green bars represent the total intercepted water by the AP, and the gold bars display the local PET estimated by the Oudin formula (ref). The hydrological inputs (mm) are calculated from the total volume (m^3), which is normalized by the watershed area (355 ha).



888

889

890

891

892

893

Figure A.3: Percentage of the mean efficiency of the Rampillon AP to reduce the concentration between the inlet and outlet (bars) of the studied pesticides. The red line represents the mean temperature T (°C) of each period and the blue line refers to the mean hydraulic residence time HRT (d) in the AP. The data is displayed according to the periods used for model validation.

6.2 Model inputs

Table A.1: List of the PESTIPOND model variables and parameters. The details on how the input data is obtained are available in (Bahi et al. 2023. submitted).

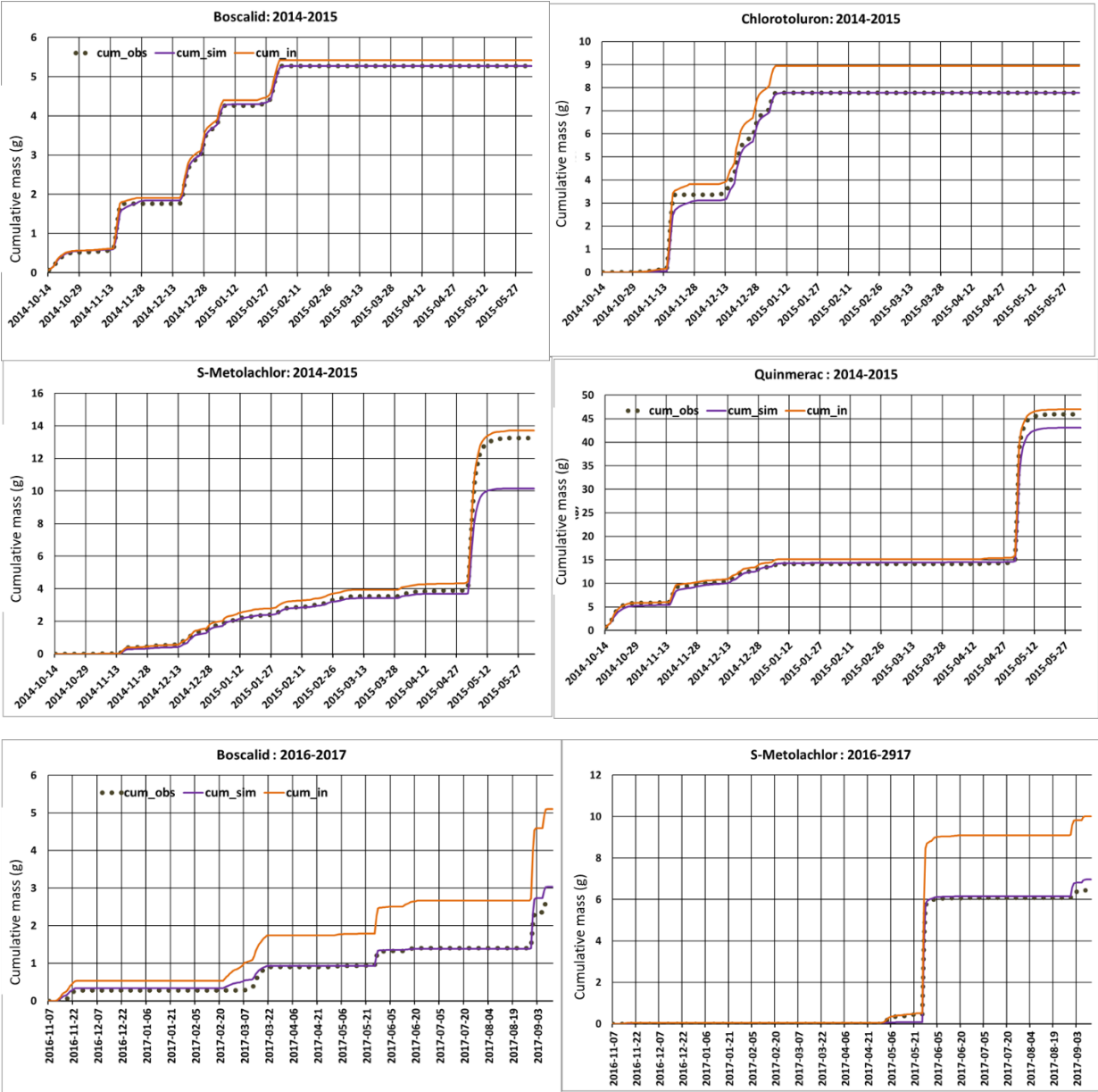
Values	Parameters	Symbol	Units
Literature/PPDB	Biotransformation in the active sediment layer	$k_{bio,s}$	T^{-1}
	Photolysis	k_p	T^{-1}
	Hydrolysis	k_h	T^{-1}
	Henry constant	H	$Pa.m^3.mol^{-1}$
	Gas constant	R	$Pa.m^3.mol^{-1}.K^{-1}$
	Mass transfer coefficient of CO_2 in water	k_{CO_2}	$M.T^{-1}$
	Mass transfer coefficient of HO_2 in water	k_{H_2O}	$M.T^{-1}$
	Molecular weight of CO_2	MW_{CO_2}	Mol
	Molecular weight of HO_2	MW_{H_2O}	Mol
	Molecular weight of the pesticide	MW	Mol
	Temperature factor	θ	Unitless
On-site measurements	Surface area of the AP	A	L^2
	Bulk density of the sediment layer	ρ_b	$M.L^{-3}$
Calibration	Adsorption kinetic coefficient	k_{ads}	T^{-1}
	Desorption kinetic coefficient	k_{des}	T^{-1}
PPDB/Calibration	Biotransformation in water	$k_{bio,w}$	T^{-1}
Forcing functions/External variables			
On-site measurements	Inlet concentration of the pesticide	$C_{in}(t)$	$M.L^{-3}$
	Inflow rate	$Q_{in}(t)$	$L^3.T^{-1}$
	Water depth	$h_w(t)$	L
	Temperature	$T(t)$	$^{\circ}C$
	Rainfall	$P(t)$	L
	Evapotranspiration	$PET(t)$	L
	Outflow rate	$Q_{out}(t)$	$L^3.T^{-1}$
Hydrological model	Water depth	$h_w(t)$	L
	Water volume	$V_w(t)$	L^3
State variables			
Model outputs	Pesticide mass in the water	$M_w(t)$	M
	Pesticide mass in the active sediment layer	$M_s(t)$	M

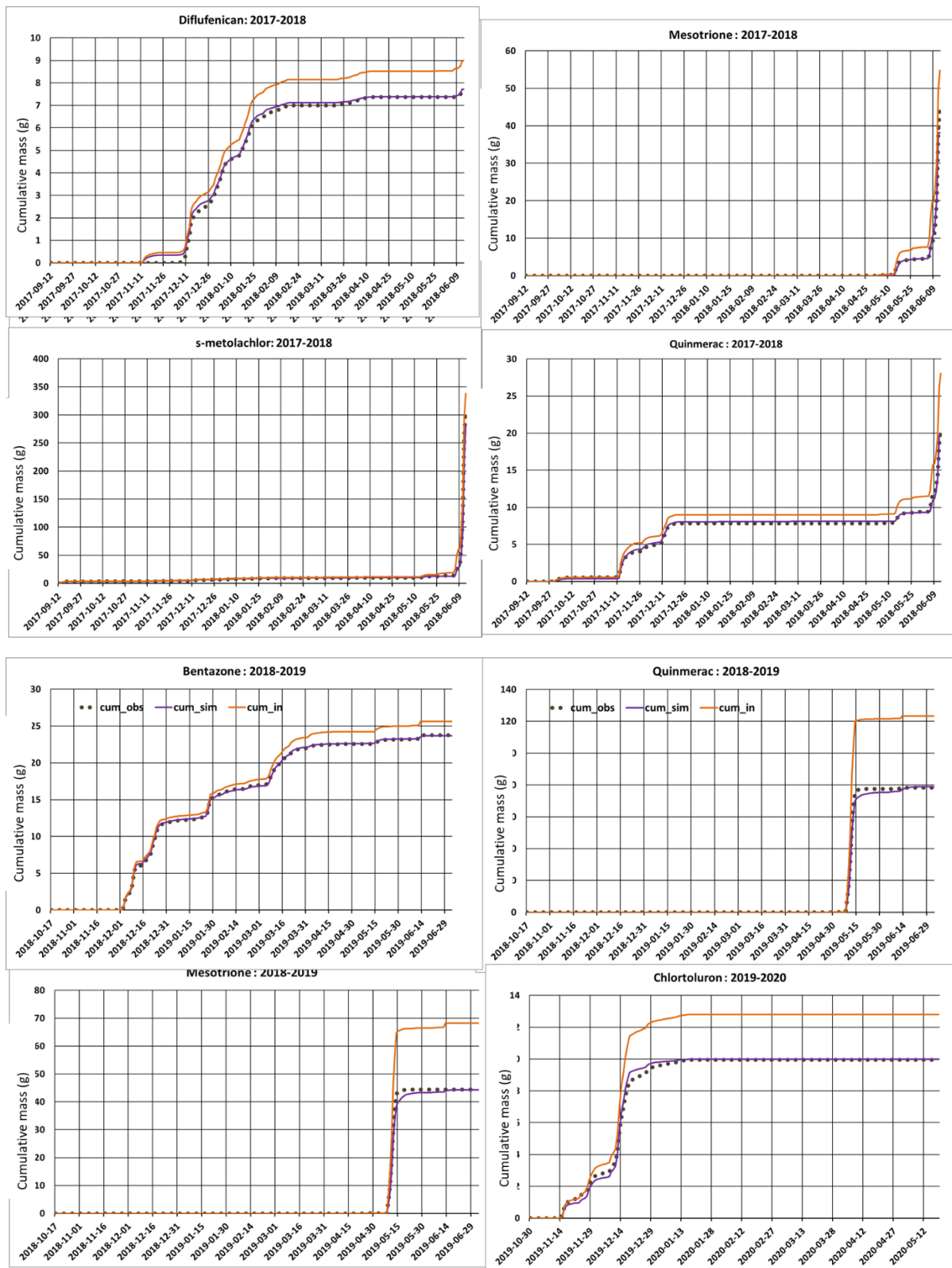
Table A.2: Values of the model parameters related to adsorption and desorption for the 20 study cases. k_{ads} (d^{-1}) and k_{des} (d^{-1}) are the adsorption and desorption kinetic coefficients, respectively. These values are the result of the annual calibration of the parameters. The set of adsorption and desorption values for the selected pesticides were calibrated because no available data was found of the literature. The calibrated values fit in the range of other studies (Comoretto et al., 2008; Nakano et al., 2004; Watanabe et al., 2006; Yoshida et al., 2000). These values are the result of the annual calibration of the parameters.

	2014-2015		2016-2017		2017-2018		2018-2019		2019-2020		PPDB	
Pesticides	k _{ads}	k _{des}	k _{ads}	k _{des}	k _{ads}	k _{des}	k _{ads}	k _{des}	k _{ads}	k _{des}	K _{oc}	log K _{ow}
Bentazone	0.19	0.015	0.2	0.015	-	-	0.11	0.015	0.11	0.015	55	2.34
Boscalid	0.06	0	1.2	0	-	-	-	-	-	-	772	3
Chlorotoluron	0.15	0	-	-	-	-	-	-	0.7	0	400	2.5
Diflufenican	0.26	0	-	-	0.27	0	-	-	1	0	550	4.2
Mesotrione	-	-	-	-	0.08	0.01	1.3	0.1	-	-	122	0.11
S-Metolachlor	0.08	0.01	0.08	0.01	0.08	0.01	-	-	0.06	0.01	120	2.9
Quinmerac	0.03	0.012	-	-	0.03	0.012	1.25	0.03	-	-	86	2.7

Table A.3: Values of the model parameters related to transformation processes, i.e., DT_{50,w} (d), DT_{50,s} (d), and DT_{50,p} (d), are the biotransformation in water, in the active sediment layer, and the photolysis half-lives, respectively. Most of transformation parameters were extracted from the PPDB and (*) are the calibrated values. Similarly to adsorption-desorption parameters, these values are the result of the annual calibration of the parameters.

	2014-2015			2016-2017			2017-2018			2018-2019			2019-2020		
Pesticides	DT _{50,w}	DT _{50,s}	DT _{50,p}	DT _{50,w}	DT _{50,s}	DT _{50,p}	DT _{50,w}	DT _{50,s}	DT _{50,p}	DT _{50,w}	DT _{50,s}	DT _{50,p}	DT _{50,w}	DT _{50,s}	DT _{50,p}
Bentazon	5	100	3	5	100	3	-	-	-	5	100	3	5	100	3
Boscalid	500*	500	stable	500*	500	stable	-	-	-	-	-	-	-	-	-
Chlorotoluron	44	300	30	-	-	-	-	-	-	-	-	-	1*	300	30
Diflufenican	200	175	133	-	-	-	200	175	133	-	-	-	200	175	133
Mesotrione	-	-	-	-	-	-	5,3	5,2	89	5,3	5,2	89	-	-	-
S-Metolachlor	1,5	43	146	1,5	43	146	1,5	43	146	-	-	-	1,5	43	146
Quinmerac	5	180	66	-	-	-	1,5*	180	66	5	180	66	-	-	-





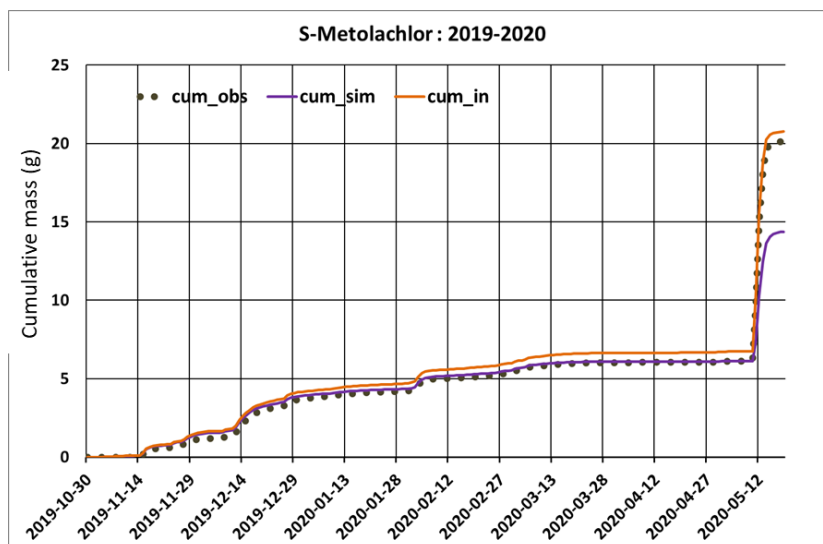


Figure A.4: Graphical comparison of simulated (purple lines) and observed (dark points) cumulative masses of the pesticides monitored during 2019-2020 in the outlet and the corresponding cumulative influx mass (orange line). cum_obs cum_sim are the cumulative masses of the observations and simulations of pesticide mass at the AP outlet using annual calibration. cum_in is the cumulative mass of the observed pesticide mass at the AP inlet. The corresponding KGE, NSE, and NRMSE are listed in Table 3.

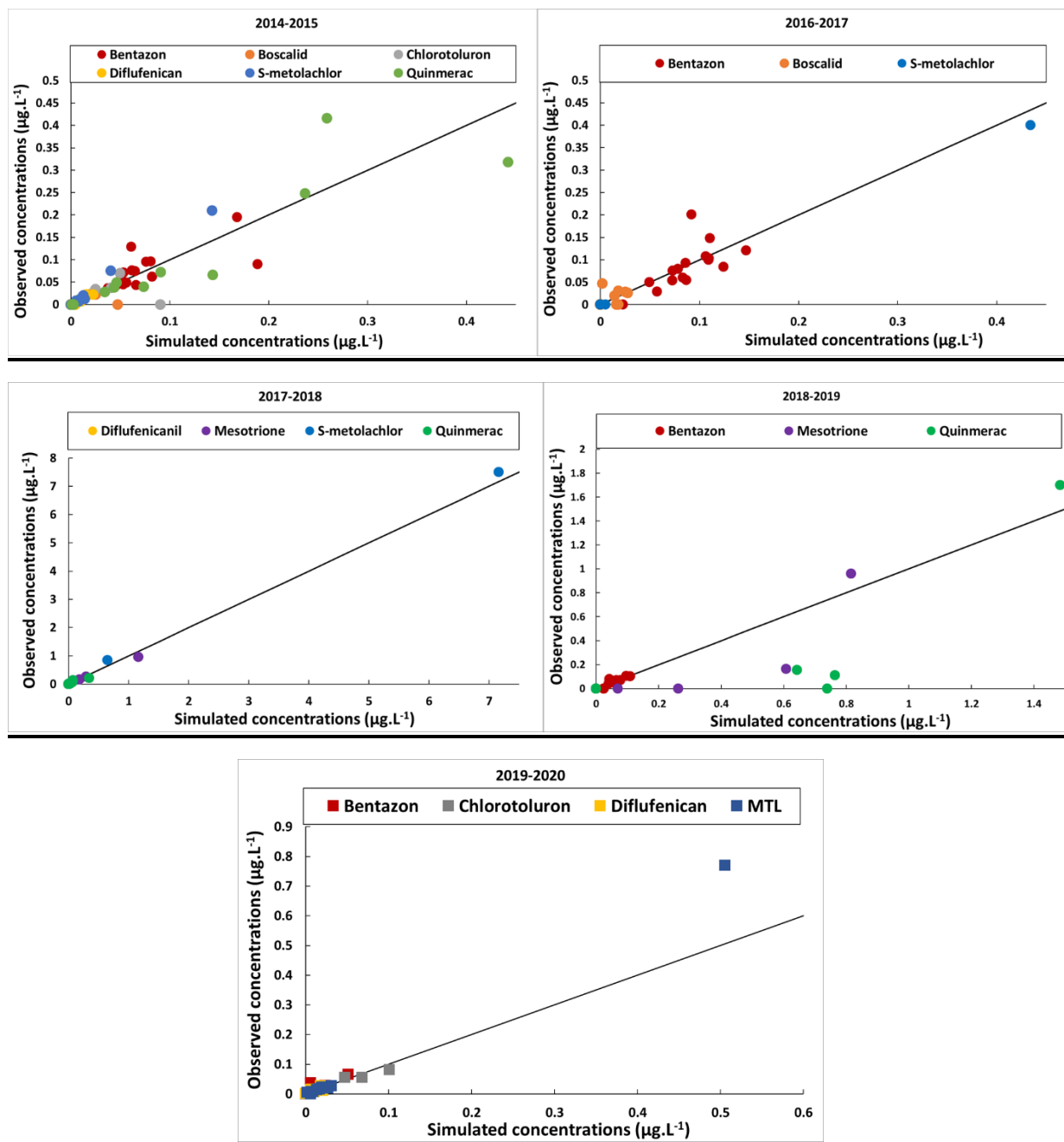
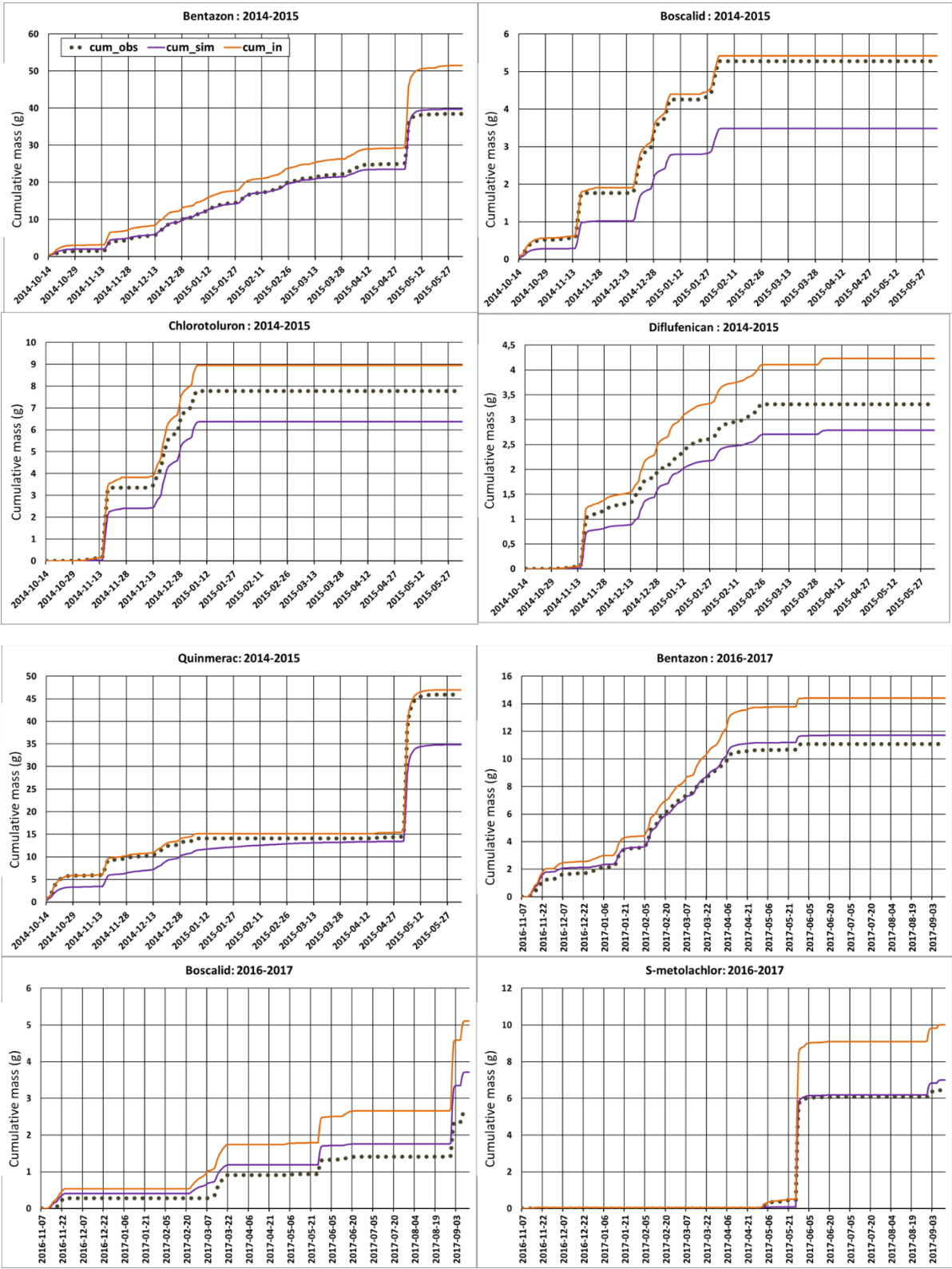
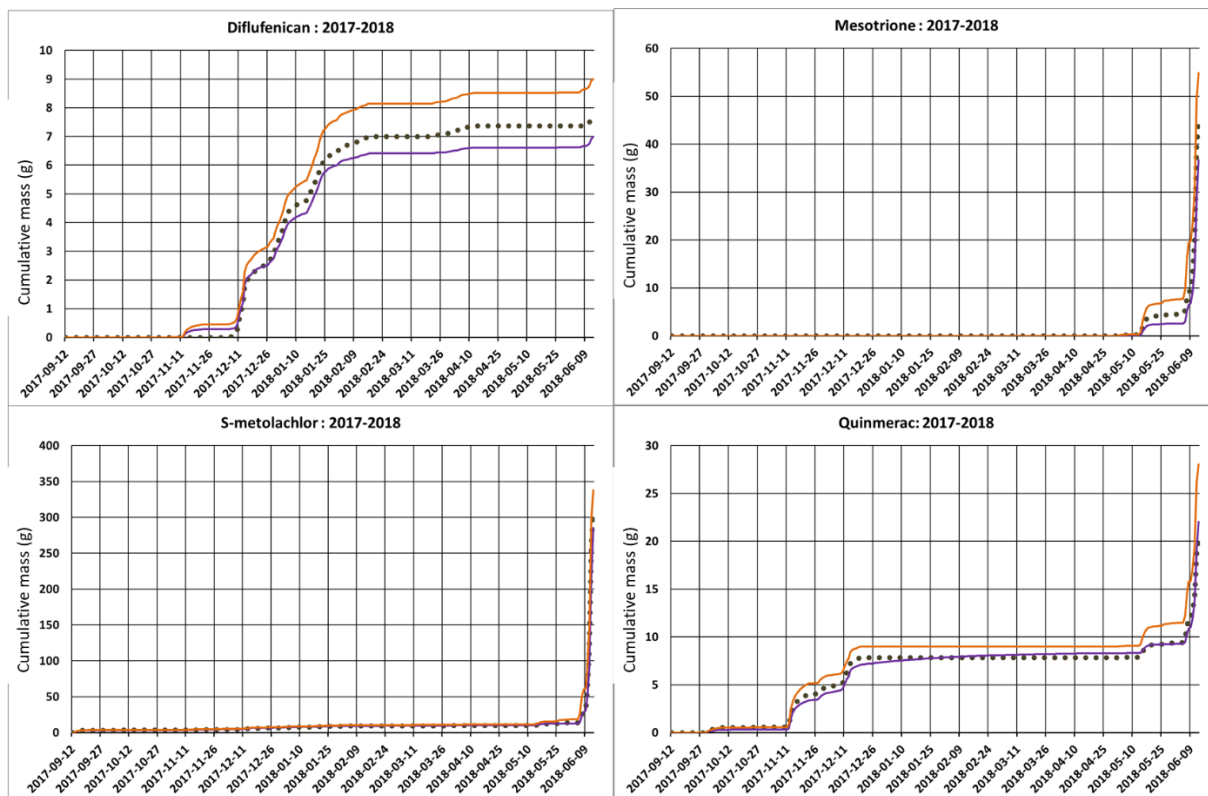
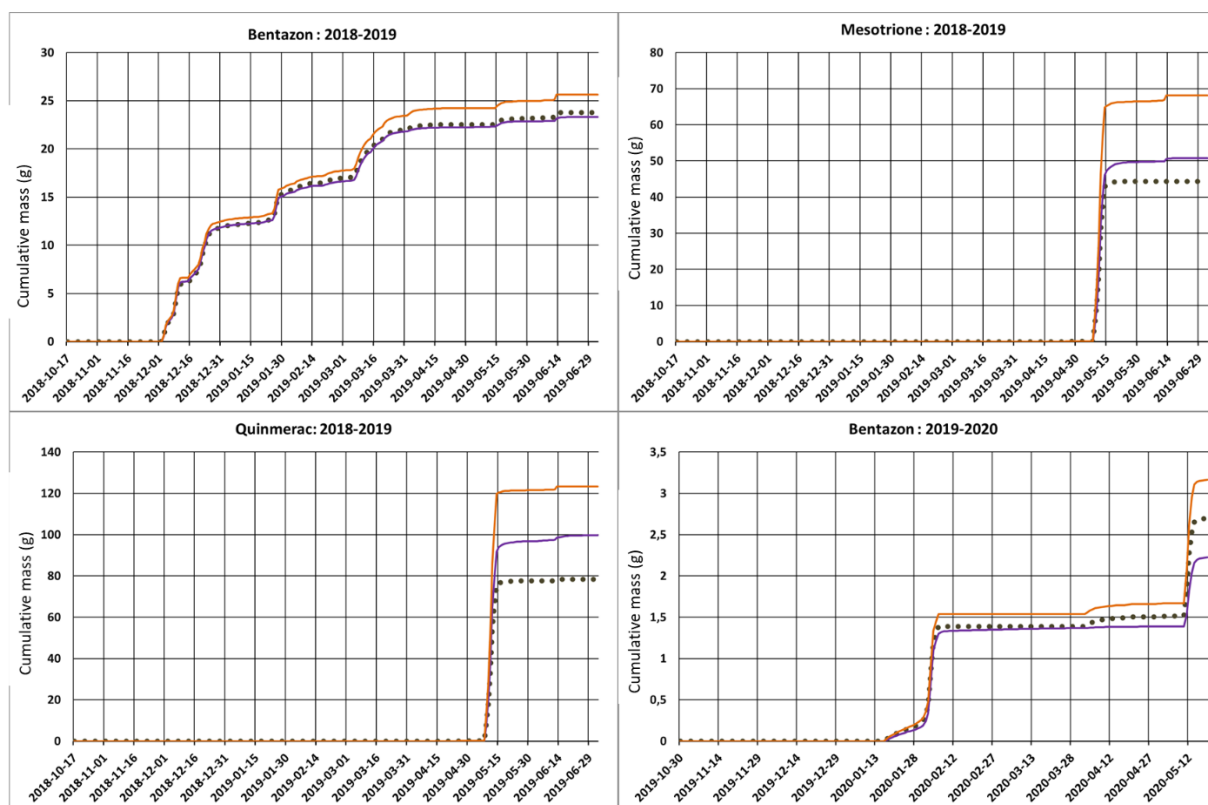


Figure A.5: Graphical comparison of the bi-monthly observations (y-axis) and simulations (x-axis) of all pesticide outlet concentrations ($\mu\text{g.L}^{-1}$) and periods combined, using the annual calibration. Each color points out a specific pesticide. The black line in the middle refers to simulations equal to observations ($y=x$).





935



936

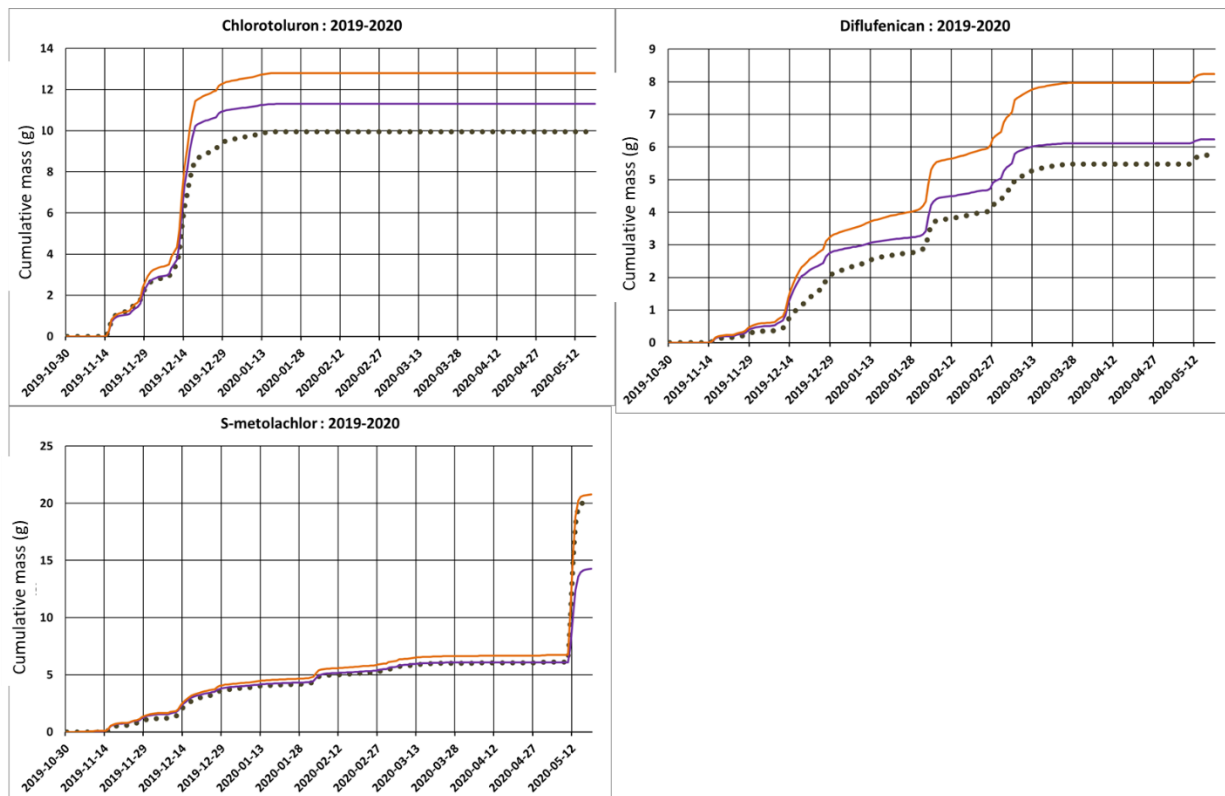


Figure A.6: Graphical comparison of simulated (purple lines) and observed (dark points) cumulative masses of pesticides in the outlet and the corresponding cumulative influx mass (orange line) for all pesticides and periods combined. The corresponding KGE, NSE, and NRMSE are listed in Table 3.

6.5 Statistical tests

Table A.4: Results of the statistical tests.

Test	2014-2015	2016-2017	2017-2018	2018-2019	2019-2020
Student's test	<i>t-value</i> : 0.40	<i>t-value</i> : 0.1	<i>t-test</i> : 0.11	<i>t-test</i> : -0.30	<i>t-test</i> : 0.18
	<i>p-value</i> : 0.68	<i>p-value</i> : 0.76	<i>p-value</i> : 0.87	<i>p-value</i> : 0.72	<i>p-value</i> : 0.81
Regression	R^2 : 0.76	R^2 : 0.41	R^2 : 0.78	R^2 : 0.85	R^2 : 0.87
	<i>p-value</i> : 7.3E-04	<i>p-value</i> : 0.01	<i>p-value</i> : 1E-08	<i>p-value</i> : 2.3E-03	<i>p-value</i> : 2.7E-04

6.6 Sorption coefficients

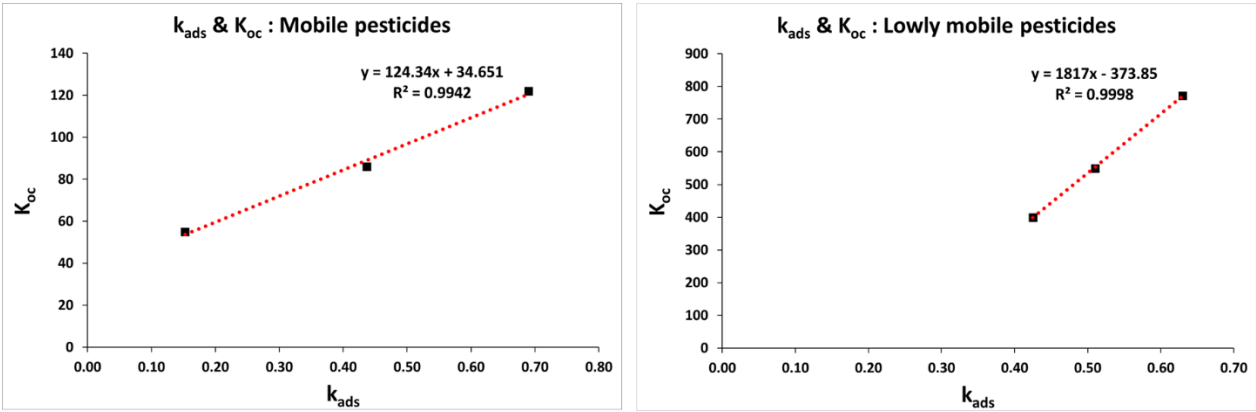


Figure A. 7 Linear correlation between the calibrated adsorption parameter (k_{ads}) and the mobility (K_{oc}) of pesticides (extracted from the PPDB (Lewis et al., 2016)). The left graph illustrates the correlation for mobile pesticides (low K_{oc}) and the right graph displays the correlation for lowly mobile pesticides (high K_{oc}).

6.7 Pesticide mass budget

Table A.5: Summary of the mass budget (g) for the studied pesticides. M_T is the total mass of the pesticide at the end of each period. M_w and M_s are the pesticide masses in water and sediments at the end of each period, respectively. $\sum M_{in}$ is the total intercepted mass. $\sum M_{out}$ the total mass discharged from the pond and $\sum M_{tr}$ is the total transformed mass. $\sum M_{tr.w}$ and $\sum M_{tr.s}$ are total transformed mass in water and sediments, respectively. $\sum M_{ads}$ and $\sum M_{des}$ are the total adsorbed and desorbed mass, respectively. Err (%) is the mass balance error of each simulation.

Pesticides	2014-2015								
	Influx/Outflux		Total mass		Transformation		Adsorption-Desorption		MBE
	$\sum M_{in}$	$\sum M_{out}$	M_w	M_s	$\sum M_{tr.w}$	$\sum M_{tr.s}$	$\sum M_{ads}$	$\sum M_{des}$	Err (%)
Bentazon	51.51	38.55	0.11	3.48	8.95	1.06	8.56	4.02	1.25
Boscalid	5.42	3.40	0.00	1.97	0.00	0.17	2.14	0.00	2.21
Chlorotoluron	8.94	6.11	0.00	2.40	0.08	0.36	2.76	0.00	0.00
Diflufenican	4.23	2.69	0.00	1.23	0.01	0.31	1.53	0.00	0.00
Mesotrione	-	-	-	-	-	-	-	-	-
S-metolachlor	13.73	9.74	0.02	0.48	3.27	0.21	1.00	0.31	0.01
Quinmerac	46.98	33.78	0.29	8.02	5.07	1.05	22.69	13.62	2.63
Mean	21.80	15.71	0.07	2.93	2.90	0.53	6.45	2.99	1.02

Pesticides	2016-2017								
	Influx/Outflux		Total mass		Transformation		Adsorption-Desorption		MBE
	$\sum M_{in}$	$\sum M_{out}$	M_w	M_s	$\sum M_{tr.w}$	$\sum M_{tr.s}$	$\sum M_{ads}$	$\sum M_{des}$	Err (%)
Bentazon	14.42	11.52	0.00	0.18	2.11	0.60	2.33	1.55	0.00
Boscalid	5.10	3.48	0.01	1.45	0.00	0.16	1.61	0.00	0.01
Chlorotoluron	-	-	-	-	-	-	-	-	-
Diflufenican	-	-	-	-	-	-	-	-	-
Mesotrione	-	-	-	-	-	-	-	-	-
S-metolachlor	10.02	6.28	0.01	0.06	3.40	0.26	0.48	0.17	0.01
Quinmerac	-	-	-	-	-	-	-	-	-
Mean	9.85	7.10	0.01	0.56	1.84	0.34	1.47	0.57	0.01

Pesticides	2017-2018								
	Influx/Outflux		Total mass		Transformation		Adsorption-Desorption		MBE
	$\sum M_{in}$	$\sum M_{out}$	M_w	M_s	$\sum M_{tr.w}$	$\sum M_{tr.s}$	$\sum M_{ads}$	$\sum M_{des}$	Err (%)
Bentazon	-	-	-	-	-	-	-	-	-
Boscalid	-	-	-	-	-	-	-	-	-
Chlorotoluron	-	-	-	-	-	-	-	-	-
Diflufenican	1.65	0.06	1.59	8.95	6.83	0.47	0.01	0.46	2.06
Mesotrione	13.52	5.36	8.15	49.52	25.64	10.35	3.11	7.25	18.65
S-metolachlor	53.88	45.97	7.92	295.85	190.05	51.91	51.30	0.61	9.11
Quinmerac	5.86	1.96	3.90	26.19	17.86	2.47	2.16	0.31	8.09
Mean	-	-	-	-	-	-	-	-	-

965

	2018-2019								
	Influx/Outflux		Total mass		Transformation		Adsorption-Desorption		MBE
	$\sum M_{in}$	$\sum M_{out}$	M_w	M_s	$\sum M_{tr.w}$	$\sum M_{tr.s}$	$\sum M_{ads}$	$\sum M_{des}$	Err (%)
Pesticides									
Bentazon	0.64	0.01	0.63	25.64	23.02	1.98	1.66	0.33	2.24
Boscalid	-	-	-	-	-	-	-	-	-
Chlorotoluron	-	-	-	-	-	-	-	-	-
Diflufenican	-	-	-	-	-	-	-	-	-
Mesotrione	0.32	0.02	0.29	68.18	49.84	18.02	2.67	15.35	26.17
S-metolachlor	-	-	-	-	-	-	-	-	-
Quinmerac	14.97	0.47	14.50	123.35	97.95	10.42	8.24	2.18	35.31
Mean	0.64	0.01	0.63	25.64	23.02	1.98	1.66	0.33	2.24

966

	2019-2020								
	Influx/Outflux		Total mass		Transformation		Adsorption-Desorption		MBE
	$\sum M_{in}$	$\sum M_{out}$	M_w	M_s	$\sum M_{tr.w}$	$\sum M_{tr.s}$	$\sum M_{ads}$	$\sum M_{des}$	Err (%)
Pesticides									
Bentazon	3.16	2.11	0.09	0.39	0.54	0.03	0.54	0.12	0.00
Boscalid	-	-	-	-	-	-	-	-	-
Chlorotoluron	12.80	11.20	0.00	1.36	0.04	0.20	1.56	0.00	0.00
Diflufenican	8.24	6.10	0.01	1.80	0.01	0.32	2.12	0.00	0.00
Mesotrione	-	-	-	-	-	-	-	-	-
S-metolachlor	20.74	13.32	0.88	1.45	4.96	0.14	1.80	0.21	0.00
Quinmerac	-	-	-	-	-	-	-	-	-
Mean	11.24	8.18	0.24	1.25	1.39	0.17	1.50	0.08	0.00

967

968 **Table A.6:** The mean percentage (%) of each process to the total intercepted/INPUT mass of pesticides.

	Photolysis	Biotransformation in water	Biotransformation in sediments	Adsorption	Desorption
Bentazon	8.68	5.21	2.14	14.63	6.82
Boscalid	0.00	0.04	3.18	35.49	0.00
Chlorotoluron	0.35	0.24	2.82	21.53	0.00
Diflufenican	0.09	0.06	5.45	28.27	0.00
Mesotrione	0.27	4.52	17.86	36.19	10.68
S-metolachlor	0.25	23.97	1.25	5.87	1.26
Quinmerac	0.46	7.94	1.70	35.26	19.32

969

970

971

972 **6.8 Extrapolation: Efficiency abacus**973 **Table A.7:** The mean efficiency (%) of the Rampillon AP according to different pond areas. A is the real AP
974 area (5270 m²).975 **Surface area = A**

	2014-2015	2016-2017	2017-2018	2018-2019	2019-2020
Bentazon	26.58	47.24	-	26.33	46.52
Chlorotoluron	29.27	-	-	-	12.52
Diflufenican	34.89	-	27.77	-	42.44
Mesotrione	-	-	48.97	52.54	-
S-metolachlor	31.42	75.19	36.59	-	50.17
Quinmerac	30.40	-	33.17	44.71	-

976

977 **Surface area = A+10 000 m²**

	2014-2015	2016-2017	2017-2018	2018-2019	2019-2020
Bentazon	50.06	71.32	-	49.49	68.90
Chlorotoluron	54.70	-	-	-	52.96
Diflufenican	60.73	-	51.86	-	67.24
Mesotrione	-	-	72.80	77.01	-
S-metolachlor	56.05	90.02	62.74	-	
Quinmerac	53.92	-	55.35	71.53	-

978

979 **Surface area = A+20 000 m²**

	2014-2015	2016-2017	2017-2018	2018-2019	2019-2020
Bentazon	61.50	80.26	-	61.47	77.84
Chlorotoluron	66.64	-	-	-	64.97
Diflufenican	71.87	-	63.81	-	76.99
Mesotrione	-	-	81.46	84.88	-
S-metolachlor	67.13	93.75	73.65	-	79.43
Quinmerac	64.13	-	65.78	80.92	-

980

981 **Surface area = A+30 000 m²**

	2014-2015	2016-2017	2017-2018	2018-2019	2019-2020
Bentazon	68.35	84.95	-	68.85	82.77
Chlorotoluron	73.58	-	-	-	72.09
Diflufenican	78.07	-	70.99	-	82.25
Mesotrione	-	-	85.94	88.74	-
S-metolachlor	73.56	95.45	79.60	-	83.75
Quinmerac	69.92	-	72.11	85.67	-

982

983

984

985

986 **Surface area = A+40 000 m²**

	2014-2015	2016-2017	2017-2018	2018-2019	2019-2020
Bentazon	72.95	87.83	-	73.85	85.89
Chlorotoluron	78.12	-	-	-	76.81
Diflufenican	82.03	-	75.80	-	85.54
Mesotrione	-	-	88.68	91.03	-
S-metolachlor	77.82	96.43	83.35	-	86.54
Quinmerac	73.67	-	76.42	88.53	-

987

988 **Surface area = A+50 000 m²**

	2014-2015	2016-2017	2017-2018	2018-2019	2019-2020
Bentazon	78.76	91.20	-	80.21	89.65
Chlorotoluron	83.71	-	-	-	82.68
Diflufenican	86.80	-	81.82	-	89.45
Mesotrione	-	-	91.85	93.62	-
S-metolachlor	83.16	97.50	87.81	-	89.95
Quinmerac	78.27	-	81.95	91.80	-

989

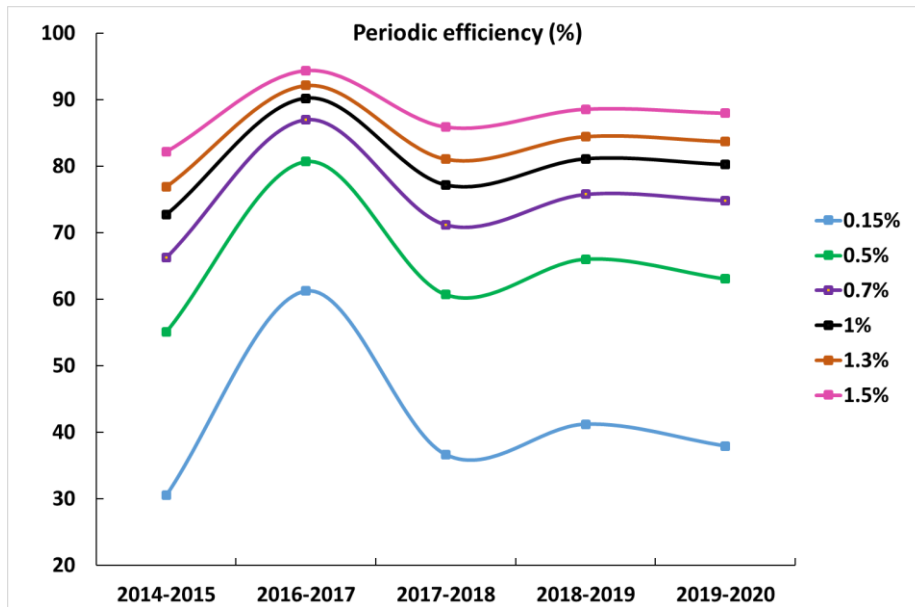


Figure A.8: The annual efficiency of the Rampillon AP to dissipate pesticides from the inlet to the outlet according to different sizes of the pond. The x-axis represents the evaluated periods and each color refers to the percentage (%) of the area occupied by the AP in the total catchment area (355ha). The actual AP area is 0.15% (5270 m²).

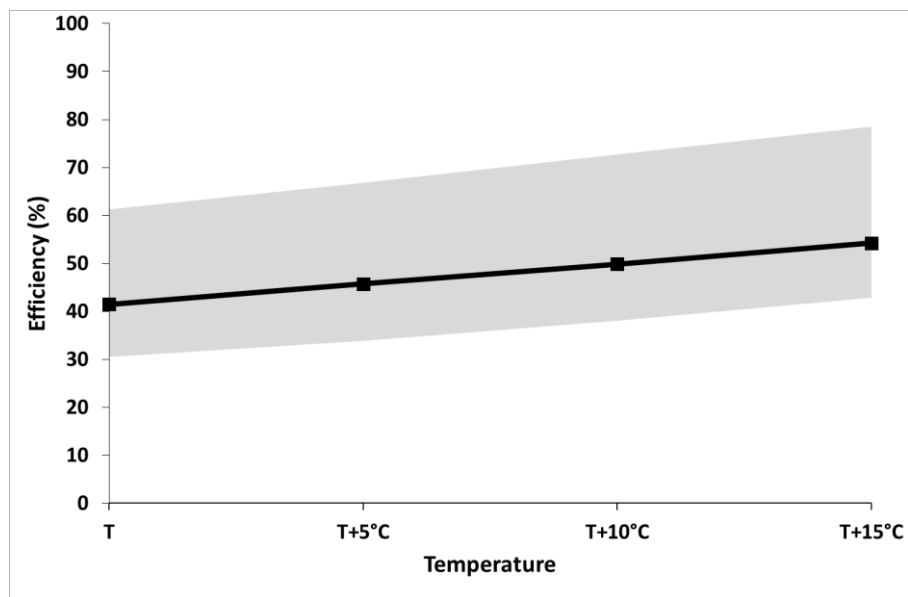


Figure A.9: The mean efficiency of the Rampillon AP to dissipate pesticides from the inlet to the outlet according to increasing temperatures. T refers to the actual daily temperature in the Rampillon AP. The upper and lower grey areas refer to the discrepancy between the mean and the maximum and minimum efficiencies, respectively.

999
1000
1001
1002
1003
1004
1005

Table A.8: Summary of pesticides monitoring data. The selected periods correspond to monitoring data without artifacts. In addition, the pesticide re-mobilization periods were not considered (i.e., pesticide outlet concentration $C_{out} > \text{inlet concentration } C_{in}$). Days refers to the total duration of each period. Q_{inmax} ($\mu\text{g.L}^{-1}$) is the maximum water flow rate intercepted by the Rampillon AP. Q_{inmean} ($\mu\text{g.L}^{-1}$) is the mean water flow rate intercepted by the Rampillon AP during the corresponding period. C_{max} ($\mu\text{g.L}^{-1}$) is the maximum detected concentration of each pesticide, C_{mean} ($\mu\text{g.L}^{-1}$) is the mean detected concentration during the corresponding period, and the DR is the detection frequency of pesticides. T ($^{\circ}\text{C}$) and HRT (d) are the average temperature and hydraulic residence time of each period, respectively. TUR (FTU) is the mean turbidity, NO_3^- (mg.L^{-1}) is the mean nitrate concentration, TOC (mg.L^{-1}) is the mean total organic carbon concentration, and DOC (mg.L^{-1}) is the mean total dissolved organic carbon concentration. Each pesticide is associated with its type: (H) Herbicides, (F) Fungicides.

Period	Duration (days)	Q_{inmax} (L.s^{-1})	Q_{inmean} (L.s^{-1})	Study case	Pesticide	C_{max} ($\mu\text{g.L}^{-1}$)	C_{mean} ($\mu\text{g.L}^{-1}$)	Detection frequency	T	HRT	TUR	NO3	TOC	DOC
14/10/2014 - 03/06/2015	233	87.44	19.45	1	Bentazon (H)	0.443	0.099	100%	8.0 5	8	8.88	10.8 7	7.53	4.03
				2	Boscalid (F)	0.064	0.029	33.30%						
				3	Chlorotoluron (H)	0.074	0.049	18.20%						
				4	Diflufenican (H)	0.026	0.01	54.50%						
				5	S-Metolachlor (H)	0.22	0.033	87.90%						
				6	Quinmerac (H)	0.921	0.238	51.50%						
07/11/2016 - 12/09/2017	310	24.2	0.73	7	Bentazon (H)	0.263	0.1106	96.80%	11. 2	14	7.98	10.6 8	6.95	4.21
				8	Boscalid (F)	0.079	0.0387	35.50%						
				9	S-Metolachlor (H)	12	1.959	19.40%						
12/09/2017 - 13/06/2018	275	147.61	27.63	10	Diflufenican (H)	0.047	0.015	58.30%	9.2	7	20.4 1	10.5 7	23.3 3	13.0 7
				11	Mesotrione (H)	1.096	0.5665	16.70%						
				12	S-Metolachlor (H)	8	0.5836	91.70%						
				13	Quinmerac (H)	0.331	0.0897	44.40%						

1006

1007 **Table A.8** (*continued*)

Period	Duration (days)	Qinmax (L.s ⁻¹)	Qinmean (L.s ⁻¹)	Study case	Pesticide	Cmax (µg.L ⁻¹)	Cmean (µg.L ⁻¹)	Detection frequency	T	HRT	TUR	NO3	TOC	DOC
17/10/2018 - 03/07/2019	260	72.32	9.95	14	Mesotrione (H)	1.449	0.5527	22.20%	8.63	9	16.8	13.2	33	20.7
				15	S-Metolachlor (H)	0.4	0.1039	44.40%						
				16	Quinmerac (H)	2.681	0.758	25.90%						
30/10/2019 - 19/05/2020	203	91.42	16.23	17	Bentazon (H)	0.082	0.0497	21.40%	8.45	6	7.1	10.2	6.4	3.7
				18	Chlorotoluron (H)	0.113	0.0757	42.90%						
				19	Diflufenican (H)	0.039	0.017	78.60%						
				20	S-Metolachlor (H)	0.77	0.0767	92.90%						

1008

1009

1010

1011

1012

7 References

- Adriaanse, P. (1996). "Fate of pesticides in field ditches: the TOXSWA simulation model." SC-DLO.
- Ahmad, R., Kookana, R. S., Megharaj, M., and Alston, A. M. (2004). Aging reduces the bioavailability of even a weakly sorbed pesticide (carbaryl) in soil. *Environ Toxicol Chem* **23**, 2084-9.
- Alvord, H. H., and Kadlec, R. H. (1996). Atrazine fate and transport in the Des Plaines Wetlands. *Ecological Modelling* **90**, 97-107.
- Aungpradit, T., Sutthivaiyakit, P., Martens, D., Sutthivaiyakit, S., and Kettrup, A. A. F. (2007). Photocatalytic degradation of triazophos in aqueous titanium dioxide suspension: Identification of intermediates and degradation pathways. *Journal of Hazardous Materials* **146**, 204-213.
- Bahi, A., Sauvage, S., Payradeau, S., and Tournebize, J. (2023a). PESTIPOND: A descriptive model of pesticide fate in artificial ponds: I. Model development. *Ecological Modelling*.
- Bahi, A., Sauvage, S., Payraudeau, S., Imfeld, G., Sánchez-Pérez, J.-M., Chaumet, B., and Tournebize, J. (2023b). Process formulations and controlling factors of pesticide dissipation in artificial ponds: A critical review. *Ecological Engineering* **186**, 106820.
- Baran, N., Lepiller, M., and Mouvet, C. (2008). Agricultural diffuse pollution in a chalk aquifer (Trois Fontaines, France): Influence of pesticide properties and hydrodynamic constraints. *Journal of Hydrology* **358**, 56-69.
- Barchanska, H., Rusek, M., and Szatkowska, A. (2012). New procedures for simultaneous determination of mesotrione and atrazine in water and soil. Comparison of the degradation processes of mesotrione and atrazine. *Environmental Monitoring and Assessment* **184**, 321-334.
- Bhardwaj, L., Sharma, S., Ranjan, A., and Jindal, T. (2019). Persistent organic pollutants in lakes of Broknes peninsula at Larsemann Hills area, East Antarctica. *Ecotoxicology* **28**, 589-596.
- Boulange, J., Kondo, K., Phong, T. K., and Watanabe, H. (2012). Analysis of parameter uncertainty and sensitivity in PCPF-1 modeling for predicting concentrations of rice herbicides. *Journal of Pesticide Science* **37**, 323-332.
- Briggs, S. A. (2018). "Basic guide to pesticides: their characteristics and hazards," CRC Press.
- Brühl, C. A., and Zaller, J. G. (2021). Indirect herbicide effects on biodiversity, ecosystem functions, and interactions with global changes. In "Herbicides", pp. 231-272. Elsevier.
- Budd, R., O'Geen, A., Goh, K. S., Bondarenko, S., and Gan, J. (2011). Removal mechanisms and fate of insecticides in constructed wetlands. *Chemosphere* **83**, 1581-7.
- Burrows, H. D., Canle, L. M., Santaballa, J. A., and Steenken, S. (2002). Reaction pathways and mechanisms of photodegradation of pesticides. *J Photochem Photobiol B* **67**, 71-108.
- Butkovskiy, A., Jing, Y., Bergheim, H., Lazar, D., Gulyaeva, K., Odenmarck, S. R., Norli, H. R., Nowak, K. M., Miltner, A., Kastner, M., and Eggen, T. (2021). Retention and distribution of pesticides in planted filter microcosms designed for treatment of agricultural surface runoff. *Sci Total Environ* **778**, 146114.
- Carsel, R. (1998). PRZM-3, a model for predicting pesticide and nitrogen fate in the crop root and unsaturated soil zones: users manual for release 3.0. <http://www.epa.gov/ceampubl/przm3.htm>.
- Catalá-Icardo, M., López-Paz, J. L., and Blázquez-Pérez, J. (2015). Development of a Photoinduced Chemiluminescent Method for the Determination of the Herbicide Quinmerac in Water. *Applied Spectroscopy* **69**, 1199-1204.
- Chaumet, B., Probst, J. L., Eon, P., Camboulive, T., Riboul, D., Payre-Suc, V., Granouillac, F., and Probst, A. (2021). Role of Pond Sediments for Trapping Pesticides in an Agricultural Catchment (Aurade, SW France): Distribution and Controlling Factors. *Water* **13**, 1734.
- Chevillard, A., Angellier-Coussy, H., Guillard, V., Bertrand, C., Gontard, N., and Gastaldi, E. (2014). Biodegradable herbicide delivery systems with slow diffusion in soil and UV protection properties. *Pest Management Science* **70**, 1697-1705.
- Comoretto, L., Arfib, B., Talva, R., Chauvelon, P., Pichaud, M., Chiron, S., and Hohener, P. (2008). Runoff of pesticides from rice fields in the Ile de Camargue (Rhône river delta, France): field study and modeling. *Environ Pollut* **151**, 486-93.

- Cryder, Z., Wolf, D., Carlan, C., and Gan, J. (2021). Removal of urban-use insecticides in a large-scale constructed wetland. *Environ Pollut* **268**, 115586.
- Desmarteau, D. A., and Ritter, A. M. (2014). Sensitivity Analysis of Individual Parameters for Synthetic Pyrethroid Exposure Assessments to Runoff, Erosion, and Drift Entry Routes for the PRZM and AGRO-2014 Models. In "Describing the Behavior and Effects of Pesticides in Urban and Agricultural Settings", Vol. 1168, pp. 287-314. American Chemical Society.
- Droz, B., Drouin, G., Maurer, L., Villette, C., Payraudeau, S., and Imfeld, G. (2021). Phase Transfer and Biodegradation of Pesticides in Water-Sediment Systems Explored by Compound-Specific Isotope Analysis and Conceptual Modeling. *Environ Sci Technol* **55**, 4720-4728.
- Edwards, C. (2013). "Environmental pollution by pesticides," Springer Science & Business Media.
- Epa, U. (2001). United States environmental protection agency. In "Quality Assurance Guidance Document-Model Quality Assurance Project Plan for the PM Ambient Air", Vol. 2, pp. 12.
- Fernández-Pascual, E., Bork, M., Hensen, B., and Lange, J. (2020). Hydrological tracers for assessing transport and dissipation processes of pesticides in a model constructed wetland system. *Hydrology and Earth System Sciences* **24**, 41-60.
- Fitch, M. W. (2014). 3.14 - Constructed Wetlands. In "Comprehensive Water Quality and Purification" (S. Ahuja, ed.), pp. 268-295. Elsevier, Waltham.
- Gobas, F., Lai, H. F., Mackay, D., Padilla, L. E., Goetz, A., and Jackson, S. H. (2018). AGRO-2014: A time dependent model for assessing the fate and food-web bioaccumulation of organic pesticides in farm ponds: Model testing and performance analysis. *Sci Total Environ* **639**, 1324-1333.
- Gregoire, C., Elsaesser, D., Huguenot, D., Lange, J., Lebeau, T., Merli, A., Mose, R., Passeport, E., Payraudeau, S., and Schütz, T. (2009). Mitigation of agricultural nonpoint-source pesticide pollution in artificial wetland ecosystems. *Environmental Chemistry Letters* **7**, 205-231.
- Gupta, H. V., Kling, H., Yilmaz, K. K., and Martinez, G. F. (2009). Decomposition of the mean squared error and NSE performance criteria: Implications for improving hydrological modelling. *Journal of Hydrology* **377**, 80-91.
- Hand, L. H., Kuet, S. F., Lane, M. C., Maund, S. J., Warinton, J. S., and Hill, I. R. (2001). Influences of aquatic plants on the fate of the pyrethroid insecticide Lambda-cyhalothrin in aquatic environments. *Environmental Toxicology and Chemistry: An International Journal* **20**, 1740-1745.
- Hantush, M. M., Kalin, L., Isik, S., and Yucekaya, A. (2013). Nutrient Dynamics in Flooded Wetlands. I: Model Development. *Journal of Hydrologic Engineering* **18**, 1709-1723.
- Henine, H., Tournebize, J., Chaumont, C., and Lemaire, B. J. (2022). Tracing and hydraulic modeling of flows in a constructed wetland for the treatment of the pollutants load from drained agricultural lands. In "IAHS-AISH Scientific Assembly 2022", Montpellier, France.
- Hunter, H. M. (2012). Nutrients and herbicides in groundwater flows to the Great Barrier Reef lagoon.
- Imfeld, G., Payraudeau, S., Tournebize, J., Sauvage, S., Macary, F., Chaumont, C., Probst, A., Sanchez-Perez, J. M., Bahi, A., Chaumet, B., Gilevska, T., Alexandre, H., and Probst, J. L. (2021). The Role of Ponds in Pesticide Dissipation at the Agricultural Catchment Scale: A Critical Review. *Water* **13**, 1202.
- Inao, K., and Kitamura, Y. (1999). Pesticide paddy field model (PADDY) for predicting pesticide concentrations in water and soil in paddy fields. *Pesticide Science* **55**, 38-46.
- Ippolito, A., Kattwinkel, M., Rasmussen, J. J., Schäfer, R. B., Fornaroli, R., and Liess, M. (2015). Modeling global distribution of agricultural insecticides in surface waters. *Environmental Pollution* **198**, 54-60.
- Jacobs, C. M. J., and Adriaanse, P. (2012). "Pesticide volatilization from small surface waters: rationale of a new parameterization for TOXSWA," Rep. No. 1566-7197. Alterra, Wageningen-UR.
- Kadlec, R. H., and Wallace, S. (2008). "Treatment wetlands," CRC press.
- Kalin, L., Hantush, M. M., Isik, S., Yucekaya, A., and Jordan, T. (2013). Nutrient Dynamics in Flooded Wetlands. II: Model Application. *Journal of Hydrologic Engineering* **18**, 1724-1738.
- Kandie, F. J., Krauss, M., Beckers, L.-M., Massei, R., Fillinger, U., Becker, J., Liess, M., Torto, B., and Brack, W. (2020). Occurrence and risk assessment of organic micropollutants in freshwater systems within the Lake Victoria South Basin, Kenya. *Science of The Total Environment* **714**, 136748.

- Kaur, J., and Vishnu (2022). Chapter 8 - Bacterial inoculants for rhizosphere engineering: Applications, current aspects, and challenges. *In* "Rhizosphere Engineering" (R. C. Dubey and P. Kumar, eds.), pp. 129-150. Academic Press.
- Kaur, P., and Kaur, P. (2018). Time and temperature dependent adsorption-desorption behaviour of pretilachlor in soil. *Ecotoxicol Environ Saf* **161**, 145-155.
- Kearns, J. P., Wellborn, L. S., Summers, R. S., and Knappe, D. R. U. (2014). 2,4-D adsorption to biochars: Effect of preparation conditions on equilibrium adsorption capacity and comparison with commercial activated carbon literature data. *Water Research* **62**, 20-28.
- Keith, L. H., and Walker, M. (1992). "EPA's pesticide fact sheet database," CRC Press.
- Kenney, J. F., and Keeping, E. (1962). Root mean square. *Mathematics of statistics* **1**, 59-60.
- Klemeš, V. (1986). Operational testing of hydrological simulation models. *Hydrological Sciences Journal* **31**, 13-24.
- Knoben, W. J. M., Freer, J. E., and Woods, R. A. (2019). Technical note: Inherent benchmark or not? Comparing Nash–Sutcliffe and Kling–Gupta efficiency scores. *Hydrology and Earth System Sciences* **23**, 4323-4331.
- Krone-Davis, P., Watson, F., Los Huertos, M., and Starner, K. (2013). Assessing pesticide reduction in constructed wetlands using a tanks-in-series model within a Bayesian framework. *Ecological Engineering* **57**, 342-352.
- Larsbo, M., and Jarvis, N. (2003). "MACRO 5.0: a model of water flow and solute transport in macroporous soil: technical description," Department of Soil Sciences, Swedish University of Agricultural Sciences Uppsala.
- Larsbo, M., Roulier, S., Stenemo, F., Kasteel, R., and Jarvis, N. (2005). An improved dual-permeability model of water flow and solute transport in the vadose zone. *Vadose Zone Journal* **4**, 398-406.
- Law, C. L., Chen, H. H. H., and Mujumdar, A. S. (2014). Food Technologies: Drying. *In* "Encyclopedia of Food Safety" (Y. Motarjemi, ed.), pp. 156-167. Academic Press, Waltham.
- Lebrun, J. D., Ayrault, S., Drouet, A., Bordier, L., Fechner, L. C., Uher, E., Chaumont, C., and Tournebize, J. (2019). Ecodynamics and bioavailability of metal contaminants in a constructed wetland within an agricultural drained catchment. *Ecological Engineering* **136**, 108-117.
- Lee, S., Gan, J., Kim, J. S., Kabashima, J. N., and Crowley, D. E. (2004). Microbial transformation of pyrethroid insecticides in aqueous and sediment phases. *Environ Toxicol Chem* **23**, 1-6.
- Lee, S., Qi, J., Kim, H., McCarty, G. W., Moglen, G. E., Anderson, M., Zhang, X., and Du, L. (2021). Utility of Remotely Sensed Evapotranspiration Products to Assess an Improved Model Structure. *Sustainability* **13**, 2375.
- Leenhardt, S., Mamy, L., Pesce, S., Sanchez, W., Achard, A.-L., Amichot, M., Artigas, J., Aviron, S., Barthélémy, C., and Beaudouin, R. (2022). Impacts des produits phytopharmaceutiques sur la biodiversité et les services écosystémiques-Résumé de l'Expertise scientifique collective-Mai 2022.
- Lemaire, B. J., Chaumont, C., Tournebize, J., and Henine, H. (2022). Tracing and hydraulic modelling of a constructed wetland. *Assemblée Internationale des Sciences Hydrologiques*.
- Lewis, K. A., Tzilivakis, J., Warner, D. J., and Green, A. (2016). An international database for pesticide risk assessments and management. *Human and Ecological Risk Assessment* **22**, 1050-1064.
- Li, Y., Zhu, G., Ng, W. J., and Tan, S. K. (2014). A review on removing pharmaceutical contaminants from wastewater by constructed wetlands: Design, performance and mechanism. *Science of The Total Environment* **468-469**, 908-932.
- Lorenz, S., Rasmussen, J. J., Süß, A., Kalettka, T., Golla, B., Horney, P., Stähler, M., Hommel, B., and Schäfer, R. B. (2017). Specifics and challenges of assessing exposure and effects of pesticides in small water bodies. *Hydrobiologia* **793**, 213-224.
- Lüdecke, D., Ben-Shachar, M. S., Patil, I., Waggoner, P., and Makowski, D. (2021). performance: An R package for assessment, comparison and testing of statistical models. *Journal of Open Source Software* **6**.
- Mahugija, J. A. M., Nambela, L., and Mmochi, A. J. (2018). Levels and distribution of pesticide residues in soil and sediments in Eastern Lake Tanganyika environs. *International Journal of Biological and Chemical Sciences* **11**, 2537.

- Materu, S. F., Heise, S., and Urban, B. (2021). Seasonal and Spatial Detection of Pesticide Residues Under Various Weather Conditions of Agricultural Areas of the Kilombero Valley Ramsar Site, Tanzania. *Frontiers in Environmental Science* **9**, 599814.
- Mergia, M. T., Weldemariam, E. D., Eklo, O. M., and Yimer, G. T. (2022). Pesticide residue levels in surface water, using a passive sampler and in the sediment along the littoral zone of Lake Ziway at selected sites. *SN Applied Sciences* **4**.
- Messelink, G. J., Lambion, J., Janssen, A., and van Rijn, P. C. (2021). Biodiversity in and around greenhouses: benefits and potential risks for pest management. *Insects* **12**, 933.
- Mineau, P., and Whiteside, M. (2013). Pesticide Acute Toxicity Is a Better Correlate of U.S. Grassland Bird Declines than Agricultural Intensification. *PLoS ONE* **8**, e57457.
- Mishra, P., Singh, U., Pandey, C. M., Mishra, P., and Pandey, G. (2019). Application of student's t-test, analysis of variance, and covariance. *Annals of cardiac anaesthesia* **22**, 407.
- Montgomery, D. C., Peck, E. A., and Vining, G. G. (2021). "Introduction to linear regression analysis," John Wiley & Sons.
- Montiel-León, J. M., Munoz, G., Vo Duy, S., Do, D. T., Vaudreuil, M.-A., Goeury, K., Guillemette, F., Amyot, M., and Sauvé, S. (2019). Widespread occurrence and spatial distribution of glyphosate, atrazine, and neonicotinoids pesticides in the St. Lawrence and tributary rivers. *Environmental Pollution* **250**, 29-39.
- Moriasi, D., Arnold, J., Van Liew, M., Bingner, R., Harmel, R. D., and Veith, T. (2007). Model Evaluation Guidelines for Systematic Quantification of Accuracy in Watershed Simulations. *Transactions of the ASABE* **50**.
- Moriasi, D., Gitau, M., Pai, N., and Daggupati, P. (2015). Hydrologic and Water Quality Models: Performance Measures and Evaluation Criteria. *Transactions of the ASABE (American Society of Agricultural and Biological Engineers)* **58**, 1763-1785.
- Motoki, Y., Iwafune, T., Seike, N., and Inao, K. (2020). Effects of temperature on the dissipation of total- and water-extractable pesticides in Japanese soils. *Journal of Pesticide Science* **45**, 86-94.
- Mulligan, R. A., Tomco, P. L., Howard, M. W., Schempp, T. T., Stewart, D. J., Stacey, P. M., Ball, D. B., and Tjeerdema, R. S. (2016). Aerobic versus Anaerobic Microbial Degradation of Clothianidin under Simulated California Rice Field Conditions. *J Agric Food Chem* **64**, 7059-67.
- Nagy, K., Duca, R. C., Lovas, S., Creta, M., Scheepers, P. T., Godderis, L., and Ádám, B. (2020). Systematic review of comparative studies assessing the toxicity of pesticide active ingredients and their product formulations. *Environmental Research* **181**, 108926.
- Nakano, Y., Yoshida, T., and Inoue, T. (2004). A study on pesticide runoff from paddy fields to a river in rural region--2: development and application of a mathematical model. *Water Res* **38**, 3023-30.
- Nash, J. E., and Sutcliffe, J. V. (1970). River flow forecasting through conceptual models part I—A discussion of principles. *Journal of hydrology* **10**, 282-290.
- Neitsch, S. L., Arnold, J. G., Kiniry, J. R., and Williams, J. R. (2011). "Soil and water assessment tool theoretical documentation version 2009." Texas Water Resources Institute.
- Nyantakyi, J. A., Wiafe, S., and Akoto, O. (2022). Seasonal Changes in Pesticide Residues in Water and Sediments from River Tano, Ghana. *Journal of Environmental and Public Health* **2022**, 1-10.
- Papaevangelou, V. A., Gikas, G. D., Vryzas, Z., and Tsihrintzis, V. A. (2017). Treatment of agricultural equipment rinsing water containing a fungicide in pilot-scale horizontal subsurface flow constructed wetlands. *Ecological Engineering* **101**, 193-200.
- Pavlidis, G., Zotou, I., Karasali, H., Marousopoulou, A., Bariamis, G., Tsihrintzis, V. A., and Nalbantis, I. (2022). Performance of Pilot-scale Constructed Floating Wetlands in the Removal of Nutrients and Pesticides. *Water Resources Management* **36**, 399-416.
- Pearson, K. (1895). Correlation coefficient. In "Royal Society Proceedings", Vol. 58, pp. 214.
- Pérez, D. J., Doucette, W. J., and Moore, M. T. (2022). Atrazine uptake, translocation, bioaccumulation and biodegradation in cattail (*Typha latifolia*) as a function of exposure time. *Chemosphere* **287**, 132104.
- Pieri, L., Bittelli, M., Wu, J. Q., Dun, S., Flanagan, D. C., Pisa, P. R., Ventura, F., and Salvatorelli, F. (2007). Using the Water Erosion Prediction Project (WEPP) model to simulate field-observed runoff and erosion in the Apennines mountain range, Italy. *Journal of hydrology* **336**, 84-97.

- PubChem (2021). National Institutes of Health (NIH). In "National Center for Biotechnology Information".
- Pugliese, L., Kusk, M., Iversen, B. V., and Kjaergaard, C. (2020). Internal hydraulics and wind effect in a surface flow constructed wetland receiving agricultural drainage water. *Ecological Engineering* **144**, 105661.
- Rani, S., and Sud, D. (2015). Effect of temperature on adsorption-desorption behaviour of triazophos in Indian soils. *Plant, soil and environment* **61**, 36-42.
- Rose, M. T., Sanchez-Bayo, F., Crossan, A. N., and Kennedy, I. R. (2006). Pesticide removal from cotton farm tailwater by a pilot-scale ponded wetland. *Chemosphere* **63**, 1849-58.
- Sarraute, S., Husson, P., and Gomes, M. C. (2019). Effect of the diffusivity on the transport and fate of pesticides in water. *International Journal of Environmental Science and Technology* **16**, 1857-1872.
- Serrano, N. (2012). Calibration strategies to validate predictive models: is new always better? *Intensive Care Medicine* **38**, 1246-1248.
- Sharifi, A., Kalin, L., Hantush, M. M., Isik, S., and Jordan, T. E. (2013). Carbon dynamics and export from flooded wetlands: A modeling approach. *Ecological Modelling* **263**, 196-210.
- Silva, G., and Ginzburg, I. (2016). Stokes–Brinkman–Darcy Solutions of Bimodal Porous Flow Across Periodic Array of Permeable Cylindrical Inclusions: Cell Model, Lubrication Theory and LBM/FEM Numerical Simulations. *Transport in Porous Media* **111**, 795-825.
- Singh, T., Awasthi, G., and Tiwari, Y. (2021). Recruiting endophytic bacteria of wetland plants to phytoremediate organic pollutants. *International Journal of Environmental Science and Technology* **19**, 9177-9188.
- Sinsomboonthong, S. (2022). Performance Comparison of New Adjusted Min-Max with Decimal Scaling and Statistical Column Normalization Methods for Artificial Neural Network Classification. *International Journal of Mathematics and Mathematical Sciences* **2022**.
- Son, Y. K., Yoon, C. G., Kim, H. C., Jang, J. H., and Lee, S. B. (2010). Determination of regression model parameter for constructed wetland using operating data. *Paddy and Water Environment* **8**, 325-332.
- Sonavane, P. G., and Munavalli, G. R. (2009). Modeling nitrogen removal in a constructed wetland treatment system. *Water Science and Technology* **60**, 301-309.
- Stokes, M., Chen, F., and Gunes, F. (2014). An introduction to Bayesian analysis with SAS/STAT® software. In "Proceedings of the SAS Global Forum 2014 Conference, SAS Institute Inc, Cary, USA (available at <https://support.sas.com/resources/papers/proceedings14/SAS400-2014.pdf>)". Citeseer.
- Sudarsan, J. S., and Nithiyanantham, S. (2021). An Integrated Constructed Wetland System for Society. pp. 397-419. Springer International Publishing.
- Takagi, K., Fajardo, F. F., Ishizaka, M., Phong, T. K., Watanabe, H., and Boulange, J. (2012). Fate and transport of bensulfuron-methyl and imazosulfuron in paddy fields: experiments and model simulation. *Paddy and Water Environment* **10**, 139-151.
- Tang, X. Y., Yang, Y., Huang, W. D., McBride, M. B., Guo, J. J., Tao, R., and Dai, Y. V. (2017). Transformation of chlorpyrifos in integrated recirculating constructed wetlands (IRCWs) as revealed by compound-specific stable isotope (CSIA) and microbial community structure analysis. *Bioresource Technology* **233**, 264-270.
- Tooby, T. (1999). FORum for the Co-ordination of pesticide fate models and their USE (FOCUS): aims and objectives. In "BRIGHTON CROP PROTECTION CONFERENCE WEEDS", Vol. 2, pp. 521-526.
- Tournebize, J., Chaumont, C., and Mander, U. (2017). Implications for constructed wetlands to mitigate nitrate and pesticide pollution in agricultural drained watersheds. *Ecological Engineering* **103**, 415-425.
- Tournebize, J., Gramaglia, C., Birmant, F., Bouarfa, S., Chaumont, C., and Vincent, B. (2012). CO-DESIGN OF CONSTRUCTED WETLANDS TO MITIGATE PESTICIDE POLLUTION IN A DRAINED CATCH-BASIN: A SOLUTION TO IMPROVE GROUNDWATER QUALITY. *Irrigation and Drainage* **61**, 75-86.

- Towner, J., Cloke, H. L., Zsoter, E., Flamig, Z., Hoch, J. M., Bazo, J., Coughlan De Perez, E., and Stephens, E. M. (2019). Assessing the performance of global hydrological models for capturing peak river flows in the Amazon basin. *Hydrology and Earth System Sciences* **23**, 3057-3080.
- Trepel, M. (2010). Assessing the cost-effectiveness of the water purification function of wetlands for environmental planning. *Ecological Complexity* **7**, 320-326.
- Tsavdaris, A., Williams, J. B., and Mitchell, S. (2013). An experimental evaluation of sustainable drainage systems. *Journal of Urban and Environmental Engineering* **7**, 206-214.
- Ulrich, U., Hörmann, G., Unger, M., Pfannerstill, M., Steinmann, F., and Fohrer, N. (2018). Lentic small water bodies: Variability of pesticide transport and transformation patterns. *Science of The Total Environment* **618**, 26-38.
- Vagi, M. C., and Petsas, A. S. (2022). Sorption/Desorption, Leaching, and Transport Behavior of Pesticides in Soils: A Review on Recent Advances and Published Scientific Research. *Pesticides in Soils: Occurrence, Fate, Control and Remediation*, 137-195.
- Vallée, R. (2015). Efficacité de zones tampons humides à réduire les teneurs en pesticides des eaux de drainage, Université de Lorraine.
- Vidal, J. P., Martin, E., Franchistéguy, L., Baillon, M., and Soubeyroux, J. M. (2010). A 50-year high-resolution atmospheric reanalysis over France with the Safran system. *International Journal of Climatology* **30**, 1627-1644.
- Vymazal, J., and Brezinova, T. (2015). The use of constructed wetlands for removal of pesticides from agricultural runoff and drainage: a review. *Environ Int* **75**, 11-20.
- Waldmann, P. (2019). On the use of the Pearson correlation coefficient for model evaluation in genome-wide prediction. *Frontiers in genetics* **10**, 899.
- Wang, Q., and Kelly, B. C. (2017). Occurrence, distribution and bioaccumulation behaviour of hydrophobic organic contaminants in a large-scale constructed wetland in Singapore. *Chemosphere* **183**, 257-265.
- Watanabe, H., and Takagi, K. (2000a). A Simulation Model for Predicting Pesticide Concentrations in Paddy Water and Surface Soil II. Model Validation and Application. *Environmental Technology* **21**, 1393-1404.
- Watanabe, H., and Takagi, K. (2000b). A Simulation Model for Predicting Pesticide Concentrations in Paddy Water and Surface Soil. I. Model Development. *Environmental Technology* **21**, 1379-1391.
- Watanabe, H., Takagi, K., and Vu, S. H. (2006). Simulation of mefenacet concentrations in paddy fields by an improved PCPF-1 model. *Pest Manag Sci* **62**, 20-9.
- Wright, M. N., Dankowski, T., and Ziegler, A. (2017). Unbiased split variable selection for random survival forests using maximally selected rank statistics. *Statistics in medicine* **36**, 1272-1284.
- Xu, L., Granger, C., Dong, H., Mao, Y., Duan, S., Li, J., and Qiang, Z. (2020). Occurrences of 29 pesticides in the Huangpu River, China: Highest ecological risk identified in Shanghai metropolitan area. *Chemosphere* **251**, 126411.
- Yoshida, T., and Nakano, Y. (2000). Behavior of pesticides in a paddy field with rapid water penetration. *Kagaku Kogaku Ronbunshu* **26**, 842-848.
- Zambrano-Bigiarini, M. (2020). Package 'hydroGOF'. *Goodness-of-fit Functions for Comparison of Simulated and Observed*.
- Zhang, D. Q., Jinadasa, K. B. S. N., Gersberg, R. M., Liu, Y., Ng, W. J., and Tan, S. K. (2014). Application of constructed wetlands for wastewater treatment in developing countries – A review of recent developments (2000–2013). *Journal of Environmental Management* **141**, 116-131.